Development of Capillary Electrophoresis-Based Methods for Analysis of Extracellular Vesicles Isolated from Cancer Cell Lines and Human Saliva

Lixuan Ren

Thesis submitted to the University of Ottawa
in partial Fulfillment of the requirements for the
Master of Science

Department of Chemistry and Biomolecular Science
Faculty of Science
University of Ottawa

Abstract

The thesis introduces two developed methods to quantify extracellular vesicles (EVs) isolated from cancer cell lines and healthy human saliva by using capillary zone electrophoresis. In the first chapter, the importance of EVs, as well as the existing EV isolation, characterization, and quantification methods, are described. The general principle of capillary electrophoresis (CE) is explained for a better understanding of these two methods.

Chapter II describes the idea and concepts of Extracellular Vesicles quantitative Capillary Electrophoresis (EVqCE). The method evolved from the previous study carried out in our research group for the quantification of viruses. After the isolation of EVs from different cell lines, the characterization and quantification of EVs were performed using nanoparticle tracking analysis (NTA) and flow cytometry. EVqCE consists of four steps for EV quantification. In this study, EVqCE was employed to know the concentrations of EVs in unknown samples, followed by calculation of the average mass of the RNA present in EVs.

In the next chapter, one of the human body fluids, i.e., saliva, was chosen for the quantification of EVs. Salivary EVqCE was developed in a similar way as EVqCE for cell lines since the general theories and procedures are practically the same. However, human saliva contains an abundant amount of viscous proteins and ribonuclease (RNase), that were the major obstacles for salivary EVs detection and quantification. The method for the isolation of EVs from the saliva was optimized, and the quantification was performed successfully. The average mass of RNA in saliva EVs was also calculated and analyzed. The concentration of saliva EVs in unknown samples were compared with the results from NTA and flow cytometry to validate the salivary EVqCE.

In the last chapter, I described the application of EVqCE to study the quality control of EVs. The method calculates the degradation level of EVs samples under different conditions, providing a potential way for real-time monitoring of the EVs status in the body fluid sample.

Acknowledgments

In the last two years of graduate study, I have received lots of valuable help from many people. Here, I would like to express my gratitude to those nice people.

First of all, my heartiest thanks to my supervisor, Professor (Dr.) Maxim Berezovski. He offered me the opportunity to study in his lab and always take care of not only my study but also my life in Canada. He always encouraged me to talk about my idea bravely and think about the question in a scientific way, which is really helpful for me. What's more, he taught me selflessly about how to manage lab work and design experiments properly and kindly helped me overcome the difficulties during my study. Without his useful guidance and insightful suggestions, I cannot finish my master's education so smoothly.

Secondly, I want to express my sincere gratitude to all the technicians who have helped me in my study. I would like to acknowledge Dr. Shahrokh Ghobadloo, who taught me the knowledge of flow cytometry and helped me with flow cytometry detection. I also want to thank Dr. Zoran Minic for teaching me a course about mass spectrometry and giving me a lot of valuable suggestions for my project. I would like to thank Dr. Yun Liu as well, who always discussed with me and helped me solve the problems on TEM patiently.

Also, I want to thank my past and present lab mates for giving me unforgettable memories. I want to thank Yaroslav Grechkin, who helped me a lot during the period when I just came to Canada. I would like to thank Dr. Prabir Kumar Kulabhusan for giving me lots of good advice, answering me many "stupid" questions, and helping me correct my first manuscript and this thesis. I also thank Emil Zaripov and Yousef Risha for their kind and patience. They are always ready to help me fix the problems. I would as well thank Vanessa Susevski and Suttinee Poolsup for their warm heart and best memory we spent together I would never forget. Nico Huttman is a nice and clever guy, we studied together, and he offered help whenever I need. I want to thank him because I learned to have a positive attitude towards everything from him. I also thank my co-worker, Yuchu Dou. Though we had some troubles before, we faced and overcame the challenges in our studies together, and I'm so happy that we all made it finally. I thank all my Chinese friends in Canada for

always making me feel at home.

Finally, I would like to extend my love and gratefulness to my mother and my boyfriend Hao Li. The support and comfort of my mom gave me much strength when I was in a tough time. For my boyfriend, I want to say that the long-distance relationship may be a huge challenge for some couples but not for us. It is all because of your exceedingly understanding, trust and love. I can’t imagine the future without you.

To my mother,

Xiaohong Wu

The best teacher and friend in my life

Table of Contents

List of Figures

List of Tables

List of Abbreviations

ABs: Apoptotic bodies

ACE: Affinity capillary electrophoresis

AFM: Atomic force microscopy

BC: Breast cancer

Borax: Sodium tetraborate

CE: Capillary electrophoresis

CFDA-SE: Carboxyfluorescein diacetate succinimidyl ester

CGE: Capillary gel electrophoresis

CIEF: Capillary isoelectric focusing

CITP: capillary isotachophoresis

CRC: Colorectal cancer

CSF: Cerebrospinal fluid

CZE: Capillary zone electrophoresis

DG: Density gradients

DLS: Dynamic light scattering

DMEM: Dulbecco's modified eagle medium

ELISA: Enzyme-linked immunosorbent protein assays

EM: Electron microscopy

EOF: Electroosmotic flow

ESCRTs: Endosomal sorting complexes required for transporter

EVqCE: Extracellular vesicles quantitative capillary electrophoresis

EVs: Extracellular vesicles

Exo: Exosome

FACS: Fluorescent-activated cell sorting

FBS: Fetal bovine serum

FSC: Forward scatter

GPC1: Glypican-1

IS: Internal standard

ISEV: The international society for extracellular vesicles

LIF: Laser-induced fluorescence

MEKC: micellar electrokinetic chromatography

MISEV: Minimal Information for studies of extracellular vesicles

MPs: Microparticles

MVB: Multi-vesicular body

MVs: Microvesicles

NECEEM: Non-equilibrium capillary electrophoresis of equilibrium mixtures

NTA: Nanoparticle tracking analysis

OSCC: Oral squamous cell carcinoma

PBS: Phosphate buffered saline

PCR: Polymerase chain reaction

PDA: Photodiode array

RNase: Ribonuclease

SDS: Sodium dodecyl sulphate

SEC: Size exclusion chromatography

SPR: Surface plasmon resonance

SSC: Side scatter

TEM: Transmission electron microscopy

UC: Ultracentrifugation

UV: Ultraviolet light

Viral qCE: viral quantitative capillary electrophoresis

%D: Degradation level

Chapter 1: Introduction

1.1 Extracellular Vesicles (EVs)

1.1.1 Overview

Extracellular vesicles (EVs) are defined as a family of spherical particles enclosed by a phospholipid bilayer released from the majority of cells to the extracellular environment. The earliest evidence for the existence of EVs shows that EVs were first observed by Peter Wolf, who had thought to study blood coagulation. In 1976, he used a series of ultracentrifugation to gather "platelet dust," some subcellular coagulant materials and then identified them by electron microscopy.[1, 2] Afterwards, the "platelet dust" has been called "microparticles" (MPs) or "microvesicles" (MVs).

EVs contain multiple components such as protein, nucleic acids, and lipids, which are very similar to their parental cells of origin. In addition, recent studies have suggested that they play an essential role in intercellular communication because EVs are shed during cell growth, activation, proliferation, senescence and apoptosis.[3-6] They could selectively pack different components, deliver "cargos" to the neighbouring and remote cells for modulating the cellular functions and changing the cell fates.[7] Such EVs have been identified from most mammalian cell types, including immune cells,[8, 9] stem cells,[10, 11] and numerous cancer cell lines.[12, 13] Additionally, these vesicles could be easily separated from most body fluids such as blood,[14] urine,[15] saliva,[16] and cerebrospinal fluid (CSF).[17] Therefore, studies on EVs and understanding their biological significance is the need of the hour.

The extracellular microenvironment of the cell contains a different subset of EVs, which can be classified based on their size, structure and biochemical properties with confusing terminologies for their nomenclature. Therefore, it is very important to provide a correct and precise classification of EVs in order to prevent the confusion and cross-contamination while isolating the specific vesicular subsets. The International

Society for Extracellular Vesicles (ISEV, https://www.isev.org) first proposed Minimal Information for Studies of Extracellular Vesicles ("MISEV") guidelines in 2014 and updated the "MISEV2014" guidelines based on the evolution of knowledge in 2018 as "MISEV2018". ISEV, a group of scientists with long-term expertise in the field of EVs biology, discussed the collection, pre-processing, separation, characterization, and functional studies of EVs in "MISEV2018". ISEV categorizes EVs based on their biogenesis and release pathway, including exosomes (Exo), ectosomes, or shedding MVs, apoptotic bodies (ABs), and other EVs subsets.[18]

1.1.2 Exosomes, Microvesicles and Apoptotic bodies

The family of EVs secreted by a single cell type could be separated into three different main groups suggested by ISEV: (1) exosomes; (2) microvesicles, also called microparticle, shedding microvesicles or ectosomes and (3) apoptotic bodies, also called apoptotic blebs.[18, 19] **Figure 1.1** demonstrated the schematic of the major pathways and origin of EVs.

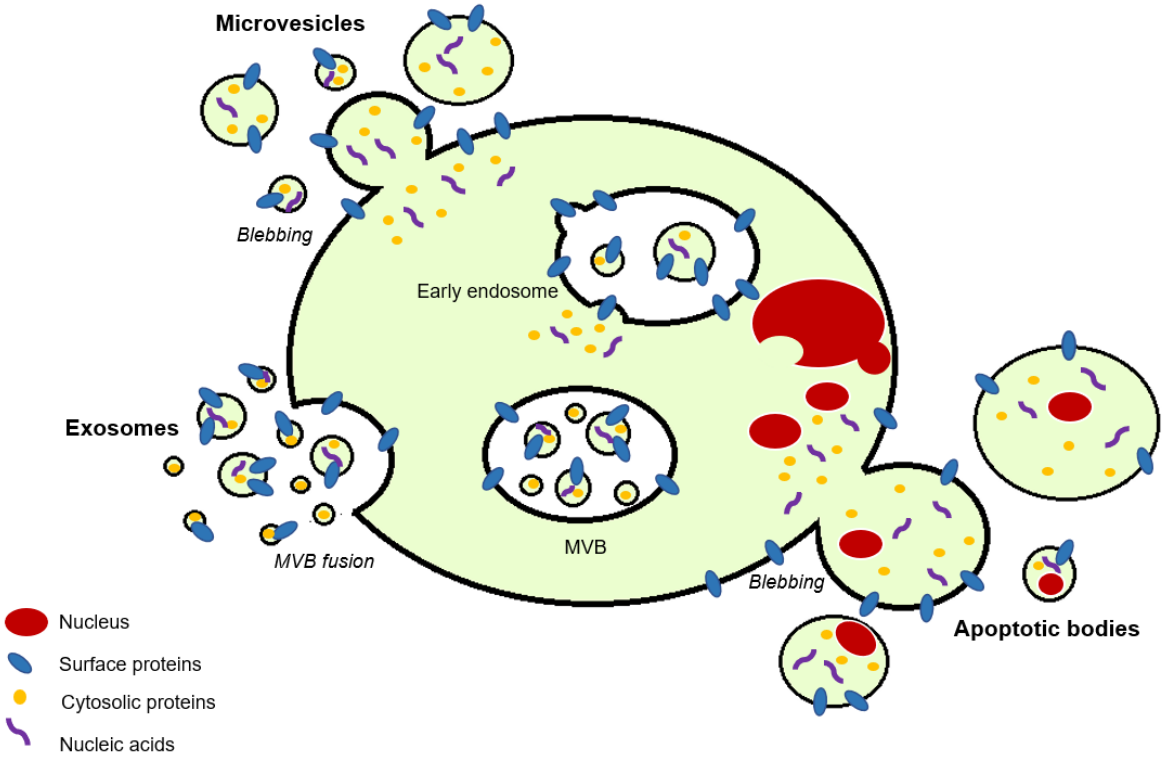

Figure 1.1 Schematic representation of the major pathways for origin and secretion of extracellular vesicles (EVs). Apoptotic bodies are generated by blebbing from cells. Microvesicles are originated directly from the plasma membrane, while exosomes are generally secreted from the fusion of multi-vesicular body (MVB) to the plasma membrane.

Exosomes (Exo) are formed within endosomal compartments and secreted by the fusion of multivesicular bodies with the plasma membrane ranged between 40 to 100 nm. They have been found in almost all biological fluid and isolated mainly from the cell cultures medium.[20] The ultracentrifugation is usually used to isolate exosomes. The Exosomes are encompassed by a phospholipid bilayer, which includes a high percentage of ceramide, cholesterol and sphingomyelin. Further, it also possesses the proteins involved in membrane transport and fusion, proteins for endosome formation such as Rab, GTPase and Annexins, and endosomal sorting complexes required for transporter (ESCRTs) and by tetraspanins, i.e., CD9, CD63 and CD81.[20-22] The tetraspanins proteins play an important role in Exo formation, which makes them the popular exosomal biomarker for the characterization technique.

Microvesicles (MVs) are generally larger than exosomes with a diameter in the range between 100 to 1000 nm. MVs are formed by budding of the plasma membrane directly and usually isolated through ultracentrifugation.[20] However, due to the size overlap, similarity in composition and lack of specific markers, the CD9 and CD63 still can be used as markers to identify MVs.

Apoptotic bodies (ABs) were first mentioned by Kerr in 1972.[23] They are released by blebbing from cells into the extracellular environment when cells are programmed to die, ranging from 50 nm to 5 μm.[20] Further, ABs are heterogeneous in shape and contain intact organelles. It also contains the histones and genomic DNA within the vesicles.[24]

Nevertheless, there still exist problems to assign individual EVs to one of the biogenesis pathways. ISEV community encouraged to include information on the physical characteristics of the EVs, biochemical composition of EVs and/or description of conditions of origin to define EV subtypes to prevent any confusion.

1.1.3 Biological Role of Extracellular Vesicles

It is becoming more and more clear that EVs have specialized functions and involved in many cellular processes. This makes people want to do more to uncover the secret of EVs. The last decade has shown a rapid increase of published papers on the topic of "EVs" (**Figure1.2 A**), indicating the mounting interest of researchers in the comprehension of this new phenomenon. The number of papers was obtained by searching the keyword "extracellular vesicles" within the Web of Science database (www.webofknowledge.com).

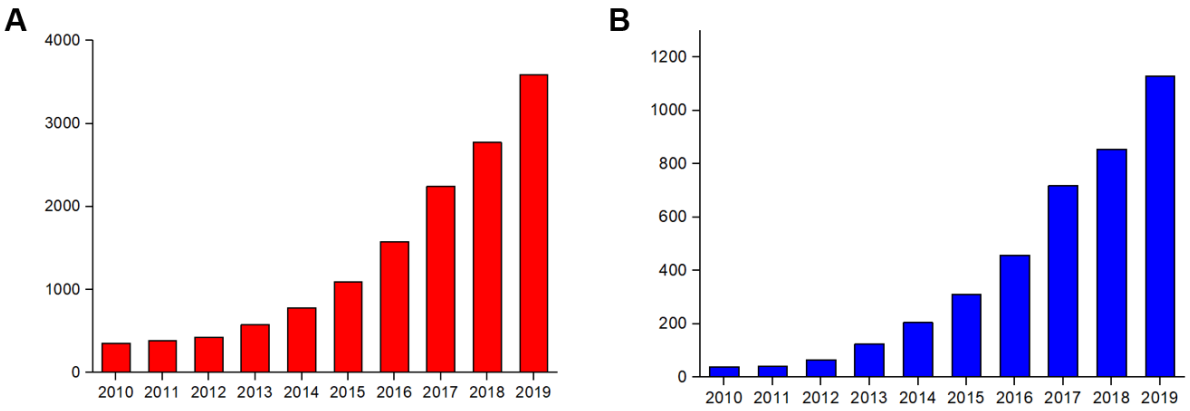

Figure 1.2 Number of papers published in the last ten years. (A) The number of papers with the keyword "extracellular vesicles" published in the last decade. (B) The number of papers published in cancer EVs research in the last ten years.

After isolating EVs, researchers realized that EVs might play key roles in many biological processes due to the components present inside. Indeed, the intercellular communication mediated by EVs has gained considerable attention, in light of the importance of understanding the multiple languages of cell-to-cell communication, especially in tumour cells and in therapy response.[25] As a matter of fact, EVs have been considered to become biomarkers, direct therapeutic targets, and engineered nanocarriers in clinical applications. Cellular interactions mediated by membrane vesicles are critical for cell growth and development as well as many pathophysiological processes, such as inflammation and immune modulation,[20, 26, 27] neuroprotection and regeneration after injury, and disease progression in central

nervous system disorders.[28] These pieces of evidence indicated that EVs might possess specific biological functions to specific target cells, actively communicating between cells. Furthermore, EVs are equipped with cell type-specific adhesion receptors and contribute to the pathogenesis of various diseases.[29] Thus, isolating EVs and analyzing their biological content could provide precious information for further studies.

Tumour cells could release membrane vesicles in Hodgkin's disease, first found by Friend and colleagues in 1978. Such membrane vesicles were described as "rare pleomorphic particles ranging from 400 to 1200 Å".[30] After 20 years, these particles, called "EVs", were proven that they are not artifacts but involved in specific phases of tumorigenesis, growth, survival and progression.[31] Moreover, cancer cells are able to communicate with each other and with normal neighbour cells in their microenvironment during the primary tumour formation through proteins and EVs.[32] Hence, studying EVs could assist scientists in understanding better of their biological role in *vivo*. In general, tumour-cell specific EVs are becoming a potential source of cancer biomarkers since they are able to transport bioactive molecules from their parental cells to other cells. In this way, EVs can promote cell migration, invasion and dissemination of cancer cells.[33]

EVs could also behave as cancer biomarkers. It has been proven that the early stages of cancer are able to be identified by the total circulating EVs. For example, exosomes containing Glypican-1 (GPC1), discovered in patients' blood, is a very sensitive and specific biomarker of pancreatic cancer.[34] From the literature, it was found that exosomes secreted from colorectal cancer (CRC), serum miR-21 is highly expressed inside, which may become a marker for early-stage diagnosis.[35] Cell-derived Exo is able to promote cancer cell proliferation through PI3K/Akt, and MAPK/ERK pathway,[36] with recent evidence, shows that CD63 has been considered as a prognostic marker for patients.[37] Moreover, in breast cancer (BC) patients, it was found that a high level of exosomal CD24 was present in serum.[38] However, CD24 could only be considered as a general marker for cancer since it is not only present in the BC but also involved in multiple cancer types.[39]

In this way, it is very clear that studying EVs from different cell lines and body fluids is important and necessary due to their unique biological roles and can provide a wealth of information about the various disease states.

1.2 Isolation of EVs

After understanding the importance of EVs, researchers design the experiments in order to learn more about these vesicles. Thus, finding the proper isolation methods of EVs should take into consideration. The different isolation methods are always related to the purity and concentration of EV samples.

Ultracentrifugation (UC). The most commonly used isolation method of EVs is ultracentrifugation. For less complex samples like cell media, it has been considered as the most efficient EV isolation technique since UC could isolate EVs directly without preliminary steps. For the isolation from complex biological fluids, UC is always followed by other methods which are able to remove specific components. The isolation of EVs relies on several centrifugation steps with different speeds to obtain the pellets of cell-debris, microvesicles and exosomes. Furthermore, UC is capable of spinning a wide range of sample volumes up to more than 100 mL. However, the isolation processes only based on different centrifugal forces, the obtained pellets would not only contain the EVs that we want but also mix with non-EV-associated proteins, particularly protein aggregates and lipoproteins.[40]

Size Exclusion Chromatography (SEC). Size exclusion chromatography is a technique to separate the EVs based upon their different sizes. This technique is able to reduce the EVs- aggregation during the isolation procedure,[41] separate EVs from soluble proteins and collect pure, intact and biologically active EVs.[42] However, a low concentration of the sample after isolation is one of the limitations of SEC, which always requires the second step to concentrate EVs by another method .[41]

Immunoaffinity. Immunoisolation is an approach that can improve the purity of EVs. Latex[14] or magnetic beads[43] are coated with specific antibodies against the surface marker of EVs and then incubate with EVs. This allows the separation of EVs based

upon the affinity of antibodies towards their marker protein. This technique could collect only EVs with the particular surface marker without any other protein contamination or other EVs populations. As compared to UC, immunoisolation shows a higher yield of EVs for the isolation of human colon cancer-derived EVs.[44] This method cannot be performed with samples of large volumes. Thus, this approach is commonly necessitating an additional purification step following conventional EVs isolation methods. However, after the elution of EVs, small changes can happen in EVs size and surface structure.[45, 46]

Density Gradients (DG) Centrifugation. The density gradient with sucrose following ultracentrifugation is most commonly used to separate EVs based on density. EVs with particular sizes and intercellular origins have a particular floatation density, ranging from 1.08 to 1.22 g/mL.[22] After UC, the EV-enriched pellet is resuspended and overlaid atop a sucrose gradient in various buffers, which may contain deuterium oxide. The appropriate fractions that enriched in EVs were collected.[47] Although sucrose gradient UC could isolate pure EVs compared to UC alone, it is considerably time-consuming. Besides, some contaminants that have a similar density like viruses,[48] lipoproteins[49] fail to separate from EVs by DG centrifugation. A high starting concentration of EVs is also required because of fractionation.[44]

1.3 Characterization of the isolated EVs

After the isolation of EVs, it is imperative to characterize the EV populations for downstream studies. There are various analytical techniques available for EVs characterization.

Electron Microscopy (EM). EM is considered an essential research tool in the discovery of apoptotic bodies, microvesicles and exosomes. EM is able to characterize these vesicles by membrane, size and shape directly on the screen of the instrument. The long time required for sample preparation, lack of multi-parametric phenotyping and low throughput capacity are the common drawbacks of transmission electron microscopy.[50] The most common TEM method used for studying EVs is by absorbing

the EVs onto a metal grid for fixation. The EVs usually are treated with negative stain before electron microscopic analysis. Chemical fixation and dehydration during sample preparation as well as damage from electron beam radiation are the reasons for a change in the size and morphology of exosomes.[51, 52] In addition, detailed parts such as surface proteins and content of vesicles are hard to be visualized by EM.

Nanoparticle Tracking Analysis (NTA). NTA was first used to study EVs in 2011.[53] This technique combines laser light scattering and Brownian motion of particles to determine their size distribution and concentration. Even though NTA allows relatively high sample throughput, its accuracy of particle size and concentration is still controversial. For example, all the particles within a certain range (around 100 nm) could be caught by the camera and counted as exosomes, which definitely contain non-exosome particles such as protein aggregates and liposomes.[50] Moreover, every time calibration is necessary before detection, and a sample needs appropriate dilution within the limits of the instrument. Particles from suspension buffers used for dilution may influence the resulting number of EVs.

Flow Cytometry. Flow cytometry has become more and more popular in EVs study recently. It is applied to identify EVs by multiparametric scattered light and fluorescence measurements.[54, 55] In fact, flow cytometry uses latex beads which have known size and with similar light-scattering properties as EVs to calibrate scatter parameters and set the related gates.[1, 56, 57] The scatter parameters include forward-scatter (FSC) and side-scatter (SSC), which could provide information about the size and density of vesicles. The sample needs to incubate with different dyes or specific fluorophore-conjugated antibodies.[58] EVs with specific protein markers or antigens can be detected, therefore allowing them to be distinguished from particles. In this way, flow cytometry is able to measure the EVs of a certain type. Further, Fluorescent-Activated Cell Sorting (FACS) could be used for identifying, gating, counting and sorting of pure EVs in any type of sample.[54, 57] Unstained samples as background need to be detected prior to stained samples for eliminating the effect of the buffer.

1.4 Quantification of the isolated EVs

A growing number of studies have demonstrated that EVs function as reliable markers of their original cells for early diagnosis of cancers. EVs could be isolated from cultured cell lines and body fluids. Nowadays, it is known that the number of EVs in biological fluids seems to have a relationship with numerous disorders and diseases. Some studies have indicated that EVs secreted from cancer cells have a higher increase rate compared to normal cells.[59-61] Thus, studying the quantification of EVs is key for the downstream analysis of EVs.

1.4.1 Physical methods to quantify EVs

Nanoparticle Tracking Analysis (NTA). As mentioned above, NTA could not only characterize EVs but also count the number of particles according to their size distribution. The advantage of this technique is less time-consuming and provides fast detection and concentration of EVs. The NTA, as a popular technique, is extensively used in EVs study; its limitation could not be ignored. The scattered light may misrepresent the data due to the existence of other sources of scattering, such as protein aggregates. Fl-NTA is an improved technique which is able to distinguish EVs from other particles better: it only tracks the objects labelled by fluorescence.[53] However, due to the limitation of the chosen fluorescent labels, Fl-NTA has not become a part of the standard characterization of EVs.[62]

Dynamic Light Scattering (DLS). DLS has the same function as NTA that could determine the size distribution of vesicles. A dispersion of diffusing EVs could scatter the laser light, causing the fluctuations of temporal intensity.[63] DLS is simple and fast, and measurements could finish in several minutes. It is best suited for quantitative analysis of relatively monodisperse samples, but as all scattering objects could be detected, DLS fails to analyze biofluids without treatment.

Atomic Force Microscopy (AFM). AFM is a type of scanning probe microscopy. It could scan the surface area with a sharp tip and translate its deflection into the height

of the surface features to image the topology.[64] Information about the mechanical properties of EVs can be offered by AFM without the requirement of sample labelling.[65] The low throughput, a requirement of specific skill sets, and costly equipment are the main limitations of this technique.

1.4.2 Chemical methods to quantify EVs

Enzyme-linked immunosorbent Sorbent Assays (ELISA). Determining the protein concentration of EVs could provide a new idea of quantifying the EVs. ELISA uses specific antibodies such as the tetraspanins, i.e., CD63, CD9 or CD81, which can only bind to common membrane proteins to capture EVs.[66, 67] High-affinity binding allows subsequent washing steps to eliminate the interference of non-EV proteins. After the antibodies labelled with enzyme bind to surface proteins of EVs, the fluorescent substrate than would interact with the enzyme, causing colour light emission for detection and quantification. The advantage of ELISA is its simplicity, and it is able to quantify EV surface proteins in complex samples like biofluids without prior EV isolation.[66, 67] However, this approach only characterizes and quantifies the specific EV subset, which is associated with target proteins.

Western Blot assay. Western blot is a common method to detect specific proteins since this assay is fast and simple. Proteins are first released from purified EVs and then separated by using SDS-PAGE. In western blot, it is mostly used to demonstrate the presence of EV-associated proteins such as CD9, CD63, Tsg101 to prove that EVs are present in the sample.[18] However, it could only be a semi-quantitative method and provide information about the whole protein contents. It also requires a large volume and a high purity of the sample.

Surface Plasmon Resonance (SPR). SPR could detect EVs by capturing them on the active surface of SPR. Gold or silver nanoparticles are normally used as SPR surface. Those nanoparticles are stabilized with DNA aptamers, which could particularly bind to the specific surface proteins of EV samples. Once the aptamers bind to EVs, the colour would change and be observed.[68] Some researchers have developed a

microfluidic SPR platform that uses a thin gold layer with nanoholes triggered by immune capture of EVs for determining the concentration of EVs.[69] This approach is highly sensitive, specific and label-free, but sensitive to buffer composition and temperature are the limitations of SPR.

1.5 Capillary Electrophoresis technique

Electrophoresis was first introduced as a separation technique in 1937. Tiselius placed a protein mixture with buffer solution in a tube which under an electric field, he found the sample components were separated and migrated in the same direction. The separation happened due to the different migration rates of components that were related to their charge and mobility. However, at the beginning of this approach, separation efficiency was limited by thermal diffusion and convection. In the early 1980s, Jorgenson and Lukacs improved the technique by using fused silica capillaries. Jorgenson described the relationship between operational parameters and separation quality,[70, 71] indicating that "high-performance" capillary electrophoresis (CE) had a high potential to be an analytical technique. From then on, CE came into the view of more and more researchers and prospered as an attractive and powerful analytical technique for further development.

A typical CE setup is shown in **Figure 1.3**. It consists of a fused silica capillary, two reservoirs filled with buffer, electrodes and a detector. Samples are injected in the capillary at the positive side (inlet) and migrate towards the negative end (outlet) hydrodynamically (by pressure). After some time, sample zones would pass by a detector (usually laser-induced fluorescence (LIF), ultraviolet light (UV), or photodiode array (PDA)), and the signal response is recorded.[72]

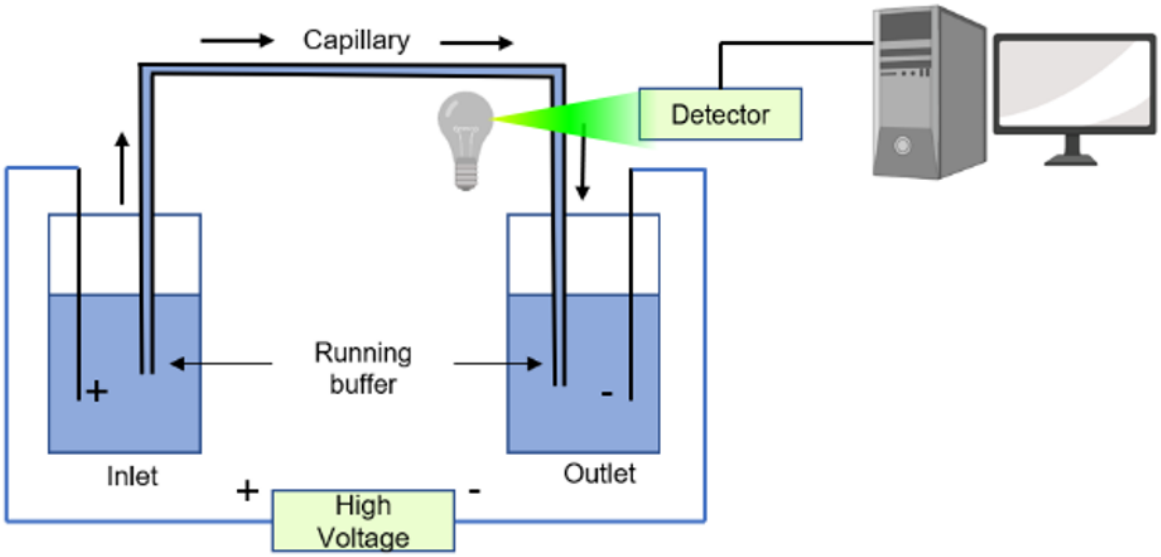

Figure 1.3 Schematic representation of a capillary electrophoresis setup. High voltage power is applied to the capillary for compounds separation. Compounds going through the narrow capillary would pass by a small detection window. The detector records signals and then transfers the data for further analysis.

There are several modes of CE designed for different analytical applications. The most common and widely used mode is capillary zone electrophoresis (CZE). Affinity CE (ACE) is a technique used to separate analytes with different affinities to a target molecule added to the separation buffer.[73] To analyze the nucleic acid sequencing, capillary gel electrophoresis (CGE) is used with a separation capillary filled with buffer containing gel. Similarly, capillary isoelectric focusing (CIEF) is a technique that uses a pH gradient to separate proteins by their isoelectric points. Other modes such as micellar electrokinetic chromatography (MEKC), capillary isotachophoresis (CITP) and non-equilibrium capillary electrophoresis of equilibrium mixtures (NECEEM) are all used in CE analysis. I used the basic mode, CZE, during my study.

CZE is a fundamental mode due to its simple operation and versatility. As shown in **Figure 1.4**, CZE could separate molecules based on their different charge to mass ratio under the electric field. The concept lies in the separation of ions according to their charge to size ratios when the analyte migrates in the buffer along the direction of the electric field. Electro-osmotic flow (EOF) is the reason for the separation of anionic, cationic and neutral solutes in CZE. EOF is the bulk flow of liquid caused by high

voltage in the capillary, and it results from the influence of the applied electric field on the solution double-layer at the interior capillary wall. Before analyzing samples, the bare fused silica capillary need wash by several steps to form a "double-layer". The capillary is first washed by NaOH to release the hydrogen ions (H^+) from silanol groups (SiOH) at inner capillary walls. In this way, the walls of the capillary become negatively charged. Subsequent washing with water and buffer is used to maintain charge balance and form the double-layer. With the application of voltage through the capillary, the second layer of cations starts moving towards the cathode. Their movements create a drag force along the wall, keeping a bulk flow of liquid in the capillary.[74]

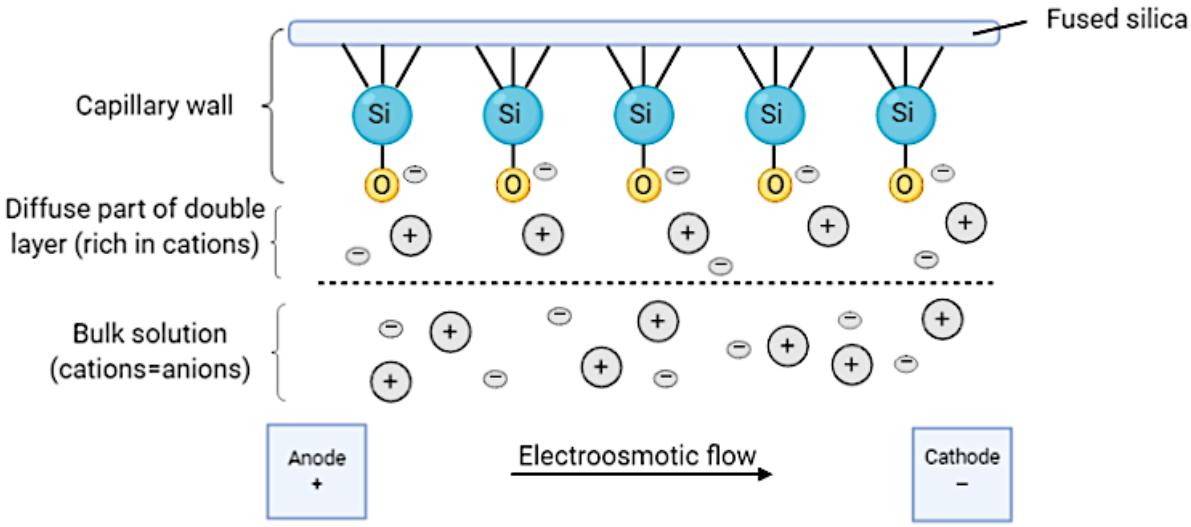

Figure 1.4 Schematics of the cross-section (inside) of a capillary. The electroosmotic flow from anode to cathode leads to the formation of the double layer and the flow of the bulk solution.

The magnitude of the EOF can be expressed in equation 1.1:

$$\boldsymbol{v}_{EOF} = \frac{(\varepsilon\zeta/\eta)}{\boldsymbol{E}} \qquad (1.2)$$

where V_{EOF} is the velocity of EOF, ε is the dielectric constant, ζ is the zeta potential, η is solution viscosity, and E is the electric field.

The zeta potential is determined by the surface charge on the capillary wall. This charge is related to pH, and the magnitude of the EOF is also changed with pH. The silanol groups are strongly deprotonated at high pH, which makes the EOF is

significantly greater than the one at low pH. The ionic strength of a separation buffer can also affect the zeta potential, where a high concentration of ions decreases the zeta potential, thus reduce EOF.

The flat profile of the flow is the unique feature of EOF in the capillary. There is no pressure drop within the capillary since the driving force of the flow is distributed along the capillary uniformly, and the flow is nearly uniform throughout. But for the laminar flow, which is affected by a pressure difference, the flow rate drops rapidly from the center of the capillary to the wall due to the shear force at the wall (**Figure 1.5**). Compared with laminar flow, EOF is able to provide narrower peaks and higher resolution.

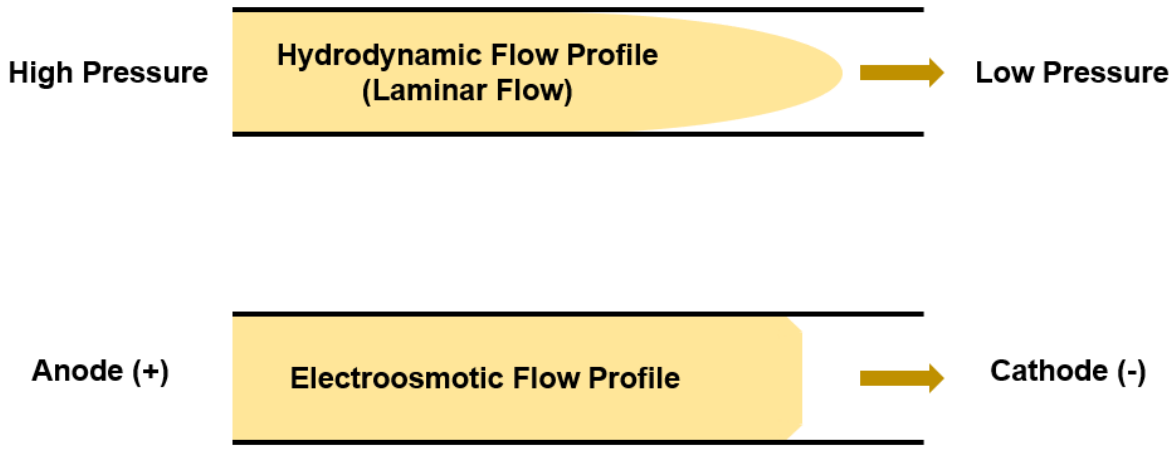

Figure 1.5 The schematics depicts the laminar flow and electroosmotic flow.

The separation happened in electrophoresis is based on the velocity (V) of different ions in an electric field. The velocity of an ion could be calculated in equation 1.2:

$$\boldsymbol{v} = \mu_e \boldsymbol{E} \tag{1.2}$$

where μ_e represents the electrophoretic mobility, and E is the applied electric field. The electric field is related to the applied voltage and capillary length. The mobility is constant for a certain ion. It is determined by the electric force and its frictional force of the ion (equation 1.3):

$$\mu_e a = \frac{\boldsymbol{Electric\ force\ (F_E)}}{\boldsymbol{Frictional\ force\ (F_F)}} \tag{1.3}$$

The electric force (F_E) can be calculated by equation 1.4:

$$\boldsymbol{F_E} = \boldsymbol{qE} \tag{1.4}$$

where q is the charge of the ion.

For a spherical ion, the frictional force can be given by equation 1.5:

$$\boldsymbol{F_F = -6\pi\eta rv} \tag{1.5}$$

where r is ion radius, and v is the velocity of ion.

When the electrophoresis is in a steady-state, the electric force and the frictional force should be equal but opposite to each other. By putting equations together and simplify them, the equation of the mobility can be written as equation 1.6:

$$\mu_e = \frac{q}{6\pi\eta r} \tag{1.6}$$

From this equation, it is shown that the species with small size and high charges would have higher mobility. In addition, under normal conditions, the flow is from the anode to the cathode. Anions will be flushed towards the cathode since the magnitude of the flow can be more than an order of magnitude greater than their electrophoretic mobilities. Therefore, cations, neutrals and anions can migrate in the same direction. Cations migrate fastest as the electrophoretic attraction, and the EOF is in the same direction, neutrals cannot be separated from each other that are only able to be carried by the EOF while anions have the lowest speed since they are attracted to the anode but are still carried by the EOF in the opposite direction (**Figure 1.6**).

Figure 1.6 Schematic representations of analytes movement in CE based on their size and charge.

CE is an instrument with many advantages. High efficiency with a small volume (~1 to 50 nL injected) and short analysis time are the key characteristics of CE. Additionally, it operates in aqueous media, which could allow the biological samples to maintain their structural integrity and morphology. It is also simple to develop methods, and once the program is set up, the instrument is able to run the sequences automatically. There are numerous modes to operates for different settings.

1.6 Research objectives

This thesis is divided into three parts. Part I (Chapter 2) introduced a new method to quantify EVs from three cancer cell lines by using CZE. In this part, differential ultra-centrifugations were utilized to collect EVs samples, and characterization techniques such as NTA, TEM and flow cytometry were performed. These techniques could provide information about the morphology, size distribution and concentration of EVs. After that, EVqCE was introduced to quantify EVs. EV samples after several steps of ultracentrifugation would contain numerous impurities such as protein aggregations, free nucleic acid fractions and lipoproteins. YOYO-1 dye was firstly added into the EVs, followed by CE separation. Species inside of the sample could be separated due to their different sizes and charges. The free nucleic acid fractions and other particles containing nucleic acids were stained by YOYO-1 and shown in an electropherogram. After lysis, the intact EVs were released inside nucleic acids, which were still stained and detected by CE. The number of lysed EVs was determined by flow cytometry. In this way, the average amount of RNA in each intact EV particles ($\bar{m}_{RNA}$) could be obtained by adding RNase after lysis. Once, $\bar{m}_{RNA}$ is quantified; the concentration of any EV sample can be calculated from the CE result. This work was done in collaboration with Yuchu Dou and Dr. Shahrokh Ghobadloo.

The results for EVs isolated from three different cancer cell lines suggested that EVqCE could be employed for the quantification of EVs. Part II of the thesis contains the application of EVqCE for the quantification of EVs isolated from the human saliva. However, salivary EVqCE shows a marginal difference in salivary EV isolation; the

integral idea of salivary EV calculation and analysis is almost the same. The results were also compared with NTA and flow cytometry to demonstrate the reliability of the developed method. This part of the work was done in collaboration with Dr. Shahrokh Ghobadloo.

The last part of this thesis describes the application of EVqCE. EV samples were degraded after sonication, vortexing, freeze-thaw and storage time. EVqCE could detect and determine different levels of degradation, which would offer great ideas to the storage and treatment of EVs in future EV researches.

Chapter 2: Extracellular vesicle quantitative capillary electrophoresis (EVqCE)

2.1 Objectives and contributions

The previous Ph.D. student in our lab, Dr. Gleb Mironov, has developed a CE-based technique, i.e., viral quantitative capillary electrophoresis (Viral qCE), which could quantify the DNA virus particles.[75] Hence, it is desirable to extend the application of this method to other natural nano-sized particles like EVs. The objective was to follow the idea of Viral qCE and develop a new method that could be suitable for EVs quantification.

Dr. Shahrokh Ghobadloo was responsible for performing flow cytometry experiments. Dr. Yun Liu was responsible for performing TEM experiments. Prof. Maxim Berezovski provided technical guidelines and supervision of CE experiments.

Yuchu Dou and I worked together, and both of us made the contribution for all the CE experiments.

2.2 Introduction

An increasing number of scientific papers in the literature have shown that EVs have significant importance in the biomedical field due to their specific functions. Moreover, some researches had already proven that EVs derived from cancer cells are different from those from healthy cells, including nucleic acids and proteins. The increase of publications with the keywords of "cancer and EVs" is evident in **Figure 1.2 B**, proving the mounting interest of researchers in this new phenomenon. In my study, I employed three different cancer cell lines, namely, MDA-MB-231, NCI-H1975 and CCL-119, to isolate, characterize and then quantify EVs by using EVqCE. The cell line MDA-MB-231 is a human breast cancer cell line that was established from a pleural effusion of a 51-year-old female with metastatic mammary adenocarcinoma.[76] The NCI-H1975

epithelial cell line was established in 1988 from a non-smoker female with lung adenocarcinoma.[77] It is useful for new lung cancer drug investigation. The derivation of the cell line CCL-119 is human lymphoblasts from peripheral blood of a 4-year-old female juvenile with acute leukemia.[78] All these three cancer cell lines were cultured and used for quantification of EVs.

In this work, I followed the idea of the original Viral qCE method and developed a new method called Extracellular Vesicles quantitative Capillary Electrophoresis (EVqCE). It is a separation-based technique that is able to discriminate between EV particles and free nucleic acids with high resolution and sensitivity. EVqCE works in a wide dynamic range of EV concentrations from 10^8 to 10^{10} particles/mL. All measurements were performed by commercial capillary electrophoresis instrument with laser-induced fluorescent detection (CE-LIF) without modifications, proving this method can be completed in less than one hour and applied in academic and industrial labs.

2.3 Materials and methods

2.3.1 Chemicals and materials

Chemicals were purchased from the following companies: sodium borate decahydrate (cat. no. SX0355-1, EMD Chemicals, U.S.A.), yeast ribonucleic acid (cat. no. 55714, Calbiochem, U.S.A), YOYO-1 Iodide (cat. no. N7565, Invitrogen, U.S.A.), sodium dodecyl sulphate (cat. no. BP166-500, Fisher Scientific), RNase A (cat. no. 21210, Affymetrix, U.S.A.), anti-human CD9 PE, clone H5C6 (cat. no. 353008), anti-human CD63 APC, clone H5C6 (cat. no. S32703), FM 5-95 (N-(3-Trimethylammoniumpropyl)-4-(6-(4-(Diethylamino)phenyl)hexatrienyl)Pyridinium Dibromide) (cat. no. T23360), UranyLess (cat. no. 22409), Triton X-100 (cat. no. T8787, Sigma-Aldrich, Canada), Tween 20 (cat. no. P9416, Sigma-Aldrich, Canada), DNase I (cat. no. EN0521, Thermo Fisher, U.S.A.). The cancer cell lines: MDA-MB-231, NCI-H1975 and CCL-119 were purchased from ATCC (U.S.A.). Dulbecco's phosphate-

buffered saline (cat. no. D8537, Sigma, U.K.), Dulbecco's modified eagle's medium-high glucose (cat. no. D5796, Sigma, U.K.), RPMI-1640 medium (cat. no. R8758, Sigma, U.K.), fetal bovine serum (cat. no. 17D192, Sigma, U.K.), antibiotic (cat. no. 15140-122, Gibco, U.S.A.). Latex beads (cat. no. 1493, ApogeeMix, U.K.) were used for flow cytometry experiments. The bare silica capillary with an outer diameter (o.d.) of 362.0 μm and an inner diameter (i.d.) of 75.3 μm was purchased from Polymicro Technologies (cat. no. TSP075375, Phoenix, AZ, U.S.A.). All buffers were prepared from nuclease-free de-ionized water using a Synergy UV water purification system supplied with a 0.22 μm filter.

2.3.2 Cell cultures

Preparation of EV free medium: EVs are present in the serum (FBS), which is generally used for routine cell culture. To avoid contamination by these EVs, the culture medium used to grow cells must be depleted of EVs. For this, 50 mL of FBS was ultracentrifuge at 100,000g for 17 h in the SW28 swinging bucket rotor (Beckman Coulter, USA). After centrifugation, the supernatants were collected slowly into a separate tube and stored at 4°C for further use. To prepare the EV free medium, i.e. the complete media, 10% of EV free FBS and 2-3% antibiotics were added and stored at 4°C for further use.

Cancer cell line MDA-MB-231 was grown in Dulbecco's modified eagle's medium-high glucose (DMEM) medium; the other two cancer cell lines, NCI-H1975 and CCL-119, were cultured in RPMI-1640 medium. The cell culture medium consisting of 10% of exosome free FBS and 2-3% antibiotic stored at 4 °C for further usage. The cells were incubated with 5% CO_2/air at 37°C. After 72 h, the cells were confluence up to 80-90%. The conditioned media was then collected in falcon tubes separately and were prepared for EVs isolation.

2.3.3 EV isolation and collection

The media from all three cell lines were subjected to the same procedures. Initially, to remove cells and the debris, the conditioned media was centrifuged at 300 g. The supernatant was collected and then centrifuged with 2,000 g at 4 °C for 30 min. The obtained pellet was which need to be discarded before the next step. Later, the supernatant was ultra-centrifuged with 100,000g at 4 °C for 3 h by using an SW28 Ti rotor (Beckman Coulter, U.S.A). In the last step, the supernatant was discarded while the pellet was washed and resuspended in 1 mL of filtered 1X PBS solution. EVs samples stored in 4 °C refrigerator. The workflow of EVs isolation and collection was schematically presented in **Figure 2.1**.

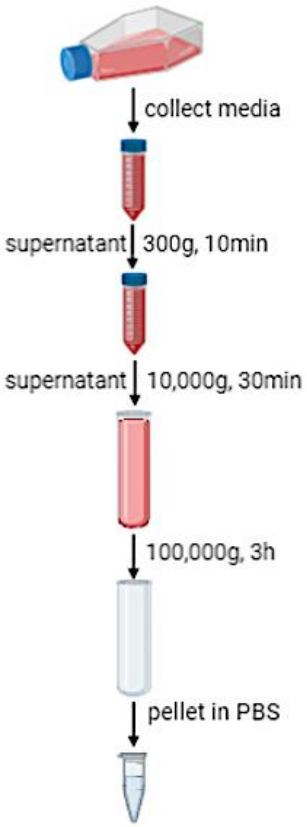

Figure 2.1 Schematic representations of the isolation process of EVs from cancer cell lines.

2.3.4 Preparation of EV samples and calibration curve

EVs samples could not be detected by CE without YOYO-1 dye. YOYO-1 (1 μL of 2 μM) was added to 49 μL of EVs samples for CE detection. The standard RNA dilutions were also stained with 1 μL of 2 μM YOYO-1 dye. The lysis of EVs was performed by using 0.1% (w/v) SDS.

For the RNA calibration curve, yeast RNA with a concentration of 0.015, 0.15, 1.5, 15, 1.5×10^2, 1.5×10^3, 1.5×10^4, 1.5×10^5 ng/mL was incubated with YOYO-1 dye separately and detected by CE.

2.3.5 Transmission electron microscopy of EVs (TEM)

For TEM characterization, a 300-mesh copper grid was first glow-discharged for 45 seconds (Solarus model 950 advanced plasma system, Gatan, U.S.A) and was covered with 10 μL of EVs samples for 5 min at room temperature. The rest of the sample was wiped away gently with a piece of filter paper. Then, the sample was stained with Uranyless negatively for 1 min. The grid was blotted using filter paper and dry in the air for at least 30 min before observation. I finished all the sample preparation work, while TEM (FEI, Tecnai Spirit) operation and sample observation were done by professional TEM technician Dr. Yun Liu.

2.3.6 Nanoparticle tracking analysis

EV samples isolated from cultured medium were analyzed by the NTA. As mentioned in the previous chapter, NTA is able to determine both particle concentration and size distribution for a certain sample at the same time. The ZetaView instrument PMX-110 (Particle Metrix, Germany) was utilized for EVs characterization. Instrument calibration was carried out using polystyrene beads ranging from 100-150 nm. The sample dilutions were performed to increase the consistency of particle counting and tracking results.

2.3.7 Flow cytometry

To date, the tetraspanins proteins (CD9, CD63 and CD81) are considered as the popular markers of EVs. Thus, flow cytometry was performed to characterize and quantify EVs through staining the EV samples with anti-human CD9, anti-human CD63 and anti-human CD81 antibodies. PBS buffer was filtered by 3 kDa (Amicon Ultra-15, Centrifugal Filter Units) to reduce the background signal. The flow cytometry instrument for EV characterization and quantification was controlled by the MoFlo Astrios EQ Cell Sorter (Beckman Coulter, U.S.A).

For EV characterization, 50 μL EV samples were diluted with PBS to 200 μL to avoid over-concentration. Subsequently, anti-human CD9 PE and anti-human CD63 APC were incubated with EVs in the dark for at least 20 min. Unstained EVs samples were also prepared in the same condition as a negative control.

For EVs quantification, all the processes were almost the same except dyes. FM 5-95 and YOYO-1 dye were used at this time. The EVs stained with dyes were incubated at least 20 min without light. Unstained samples were used as a control to correct for the effect of the background.

Samples were prepared by Yuchu Dou and me, all the flow cytometry operations were done under the guidance of Dr. Shahrokh Ghobadloo. The flow cytometry data were analyzed by Kaluza software by myself.

2.3.8 Capillary electrophoresis

All CE experiments were performed on a PA800 plus pharmaceutical analysis capillary electrophoresis system (Beckman Coulter, Brea, U.S.A) with a LIF detector. Fluorescence was excited with a 488-nm line of an Ar-ion laser and detected at 520 ± 10 nm. A bare silica-fused capillary of 59 cm length, with 49 cm from an injection point to a detection window, was used for separation. A plug of 50 nL sample was injected into the capillary by applying a pressure pulse of 1.0 psi for 5 seconds. The analytes in the sample were separated by applying 25 kV potential difference along the capillary

resulting in an electric field of 424 V/cm. The capillary temperature was maintained at 15 °C all the time.

The run buffer of 25 mM sodium tetraborate (borax) at pH 9.0 was used for the CE experiments. Before each injection, the capillary was rinsed with 0.1 M HCl for 2 min, 0.1 M NaOH for 2 min, ddH_2O for 2 min and 25 mM borax for 2 min. All solutions were filtered through a 0.2 μm membrane before use. The recording of the electropherogram and the data were analyzed using 32 Karat software. Finally, Microsoft-Excel and Origin 9.0 software were used to calculate the results.

2.4 Results and discussion

2.4.1 Characterization of EVs

TEM. TEM is a technique that is capable of visualizing the EV particles directly. Uranyless is a new stain solution that has been tested on many biological samples as an easier and safer biological staining for TEM. Thus, it is a good substitute to uranyl acetate with similar results. It is able to distinguish EV particles from other impurities by three aspects: size, shape and membrane. The particles with bilayer membrane and round shape, ranging from 50 nm to 200 nm, are recognized as EVs. The images of EVs from three cell lines are demonstrated in **Figure 2.3**. The purity of our EV samples was very low, as lots of particles and contaminations are visible.

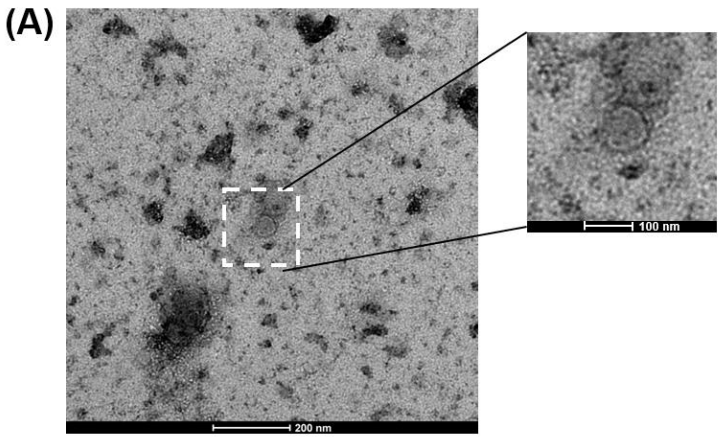

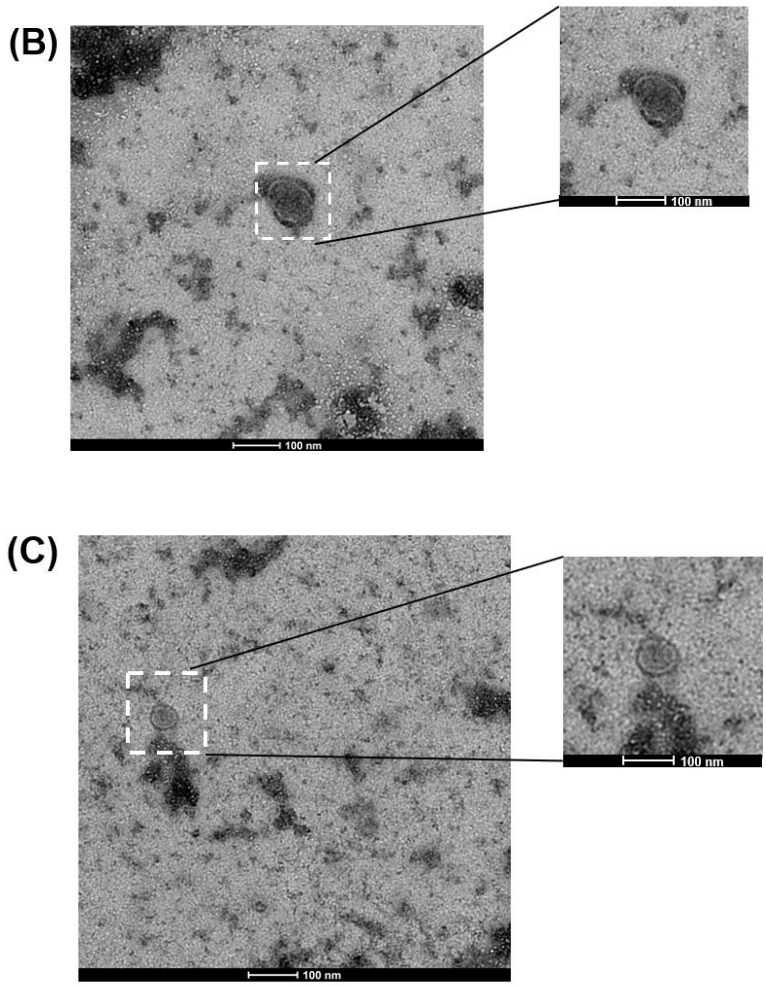

Figure 2.2 Images of transmission electron microscopy of three cell lines. (A) TEM result of EVs isolated from the MDA-MB-231 cell line. (B) TEM result of EVs isolated from the NCI-H1975 cell line. (C) TEM result of EVs isolated from the CCL-119 cell line. All the samples were stained negatively with UranyLess for 1 min.

NTA. NTA is a common technique that could provide information about both the size distribution and concentration of particles in a sample. Most EV samples were diluted a thousand times (1000x) for NTA detection. The size distributions of EVs from MDA-MB-231, NCI-H1975 and CCL-119 are presented in **Figure 2.2**. From the results, we can see that particles with the size of 187.0 nm are abundant in MDA-MB-231 cell line samples, while the size of most particles in NCI-H1975 and CCL-119 cell line samples are 158.7 nm and 139.3 nm, respectively. The concentrations of the three cell line EV samples are 4.8 $\times 10^9$ particles/mL, 2.3 $\times 10^9$ particles/mL and 2.9 $\times 10^9$ particles/mL, which are presented in **Table 2.1** for comparison with other methods. NTA could only prove that most particles in the samples ranged from 50 to 500 nm, but obviously, not

all the observed particles are EVs. Thus, it can be concluded that more experiments are required to characterize EVs.

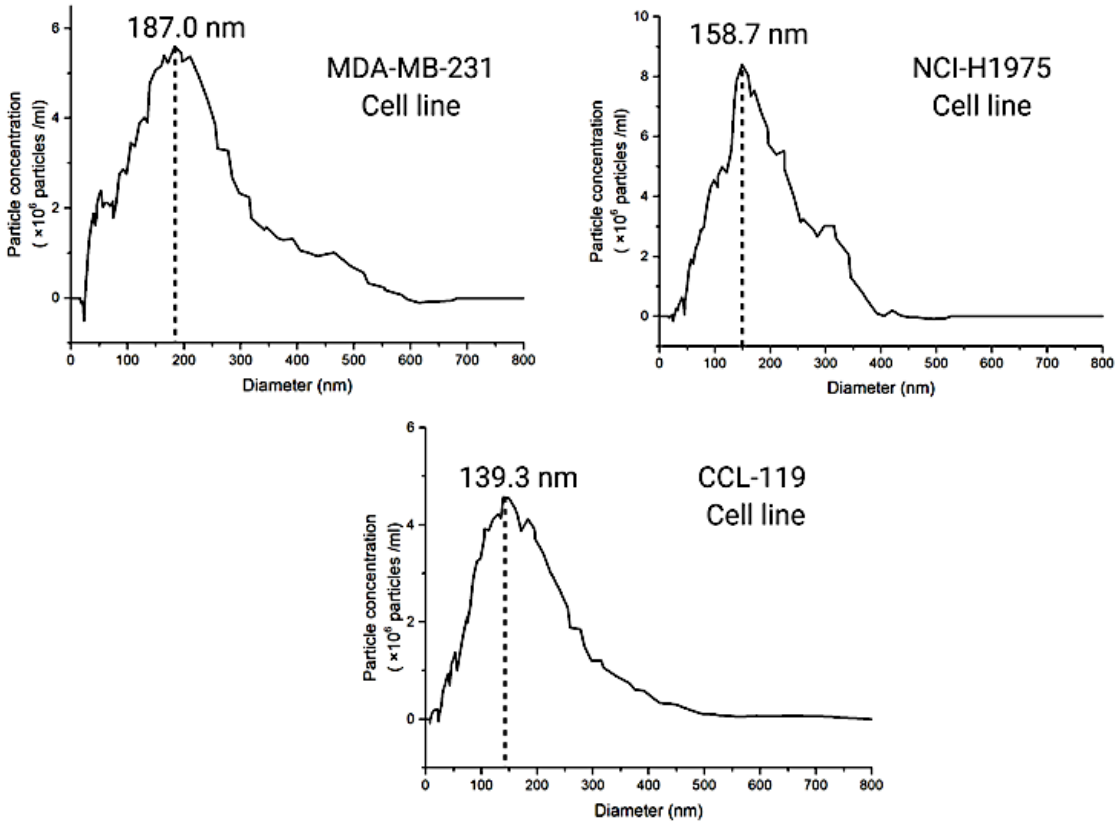

Figure 2.3 The results of nanoparticle tracking analysis of three cell lines. Size distributions of EVs from three different cell lines, MDA-MB-231, NCI-H1975 and CCL-119, respectively, are presented. The size of the most abundant particles in the sample is depicted with the dotted line.

Flow cytometry. Flow cytometry could use chemical materials for EV characterization. It is clear that the tetraspanin family (CD63, CD81, CD9) is the popular biomarkers of EVs. Hence, anti-human CD63 APC and anti-human CD9 PE, dye-conjugated antibodies, were chosen to incubate with the samples. Particles showing double-positive with two antibodies were identified as EVs as well as the percentage of double-positive particles also indicates the amount of EVs in the sample. From flow cytometry data in **Figure 2.4**, the existence of EVs is very clear, and about 20-45% of vesicles in the samples are EVs.

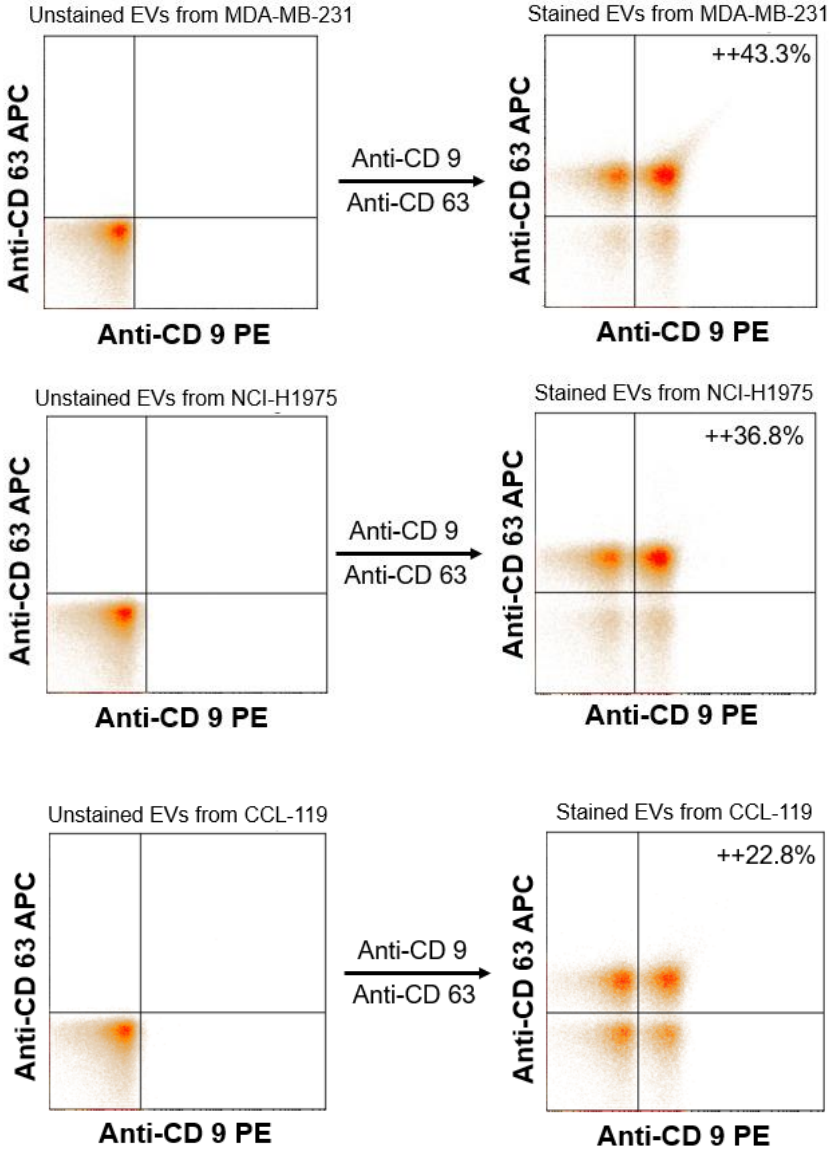

Figure 2.4 The results of flow cytometry for EVs characterization. Samples isolated from MDA-MB-231, NCI-H1975 and CCL-119 cell media were stained with anti-CD9 PE and anti-CD63 APC to prove the existence of EVs. The percentage of particles in the double-positive area is in the range from 20% to 45%.

2.4.2 CE analysis of EVs

The general principle of the new method EVqCE is shown in **Figure 2.5**. After EV isolation and collection, the EV sample contains lots of species such as intact EV particles, disintegrated EV particles, protein complex and free nucleic acids, which were either released from broken EVs or existed in the original sample. When the

sample was subjected to analysis, the CE will separate all kinds of particles based on their differential mobilities. YOYO-1 dye, which can only stain nucleic acids, was chosen to incubate with each EV sample. In this way, two kinds of analytes can be visualized in the electropherogram: intact or disintegrated EV particles and free nucleic acids. In electropherograms, two distinct zones were observed (**Figure 2.5 A**) where the fast-moving zone contains intact or disintegrated EV particles showing a bunch of sharp peaks, and the slow-moving zone contains free nucleic acids as a wide peak. The reason why EV particles travel faster than free nucleic acids is that these particles have smaller charge and bigger size. After EV lysis, the sharp peaks, which represent EV particles, would disappear, and the wide peak would increase as the interior nucleic acids are released from EVs and become free nucleic acids (**Figure 2.5 B**).

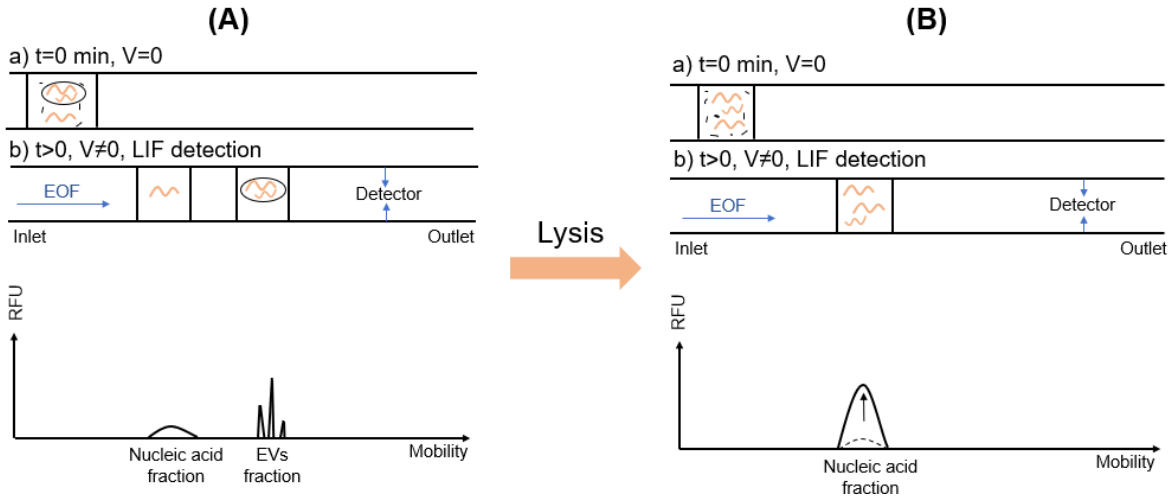

Figure 2.5 Schematic representation of the general principle of EVqCE. (A) The EV sample before lysis is injected into the capillary. CE could separate EVs fraction and free nucleic acids after sample staining with YOYO-1 in capillary under the electric field. (B) After EVs were lysed, the interior RNA and DNA were released. Thus, the peaks of EVs fraction disappear and the peak of free nucleic acid increases.

The control experiments were performed by running an EV sample without YOYO-1 and a sample of YOYO-1 dye alone, which demonstrated that the EV sample and YOYO-1 do not have auto-fluorescence (**Figure 2.6 A and B**). From **Figure 2.6 C and D,** we can see, the results of EVs stained with YOYO-1 before and after lysis are consistent with the working principle where two distinctive zones represent EVs fraction and nucleic acid fraction, respectively.

To validate the wide peak is a free nucleic acid fraction, RNase A and DNase I were added into the EV samples stained with YOYO-1 after lysis. The intense decrease of the wide peak observed after the addition of RNase A (**Figure 2.6 E**) means RNA is the most abundant nucleic acid contained in EV particles. In addition, the migration time of standard RNA is the same as one of the wide peaks, which could also provide another evidence for the presence of nucleic acid (**Figure 2.6 F**).

EVs isolated from MDA-MB-231, NCI-H1975 and CCL-119 cell lines were all detected by CE, whereas **Figure 2.6** only demonstrates the results of EVs collected from MDA-MB-231 cell media. The results of the other two cell lines are similar, which are shown in the supplementary information (Figure S2).

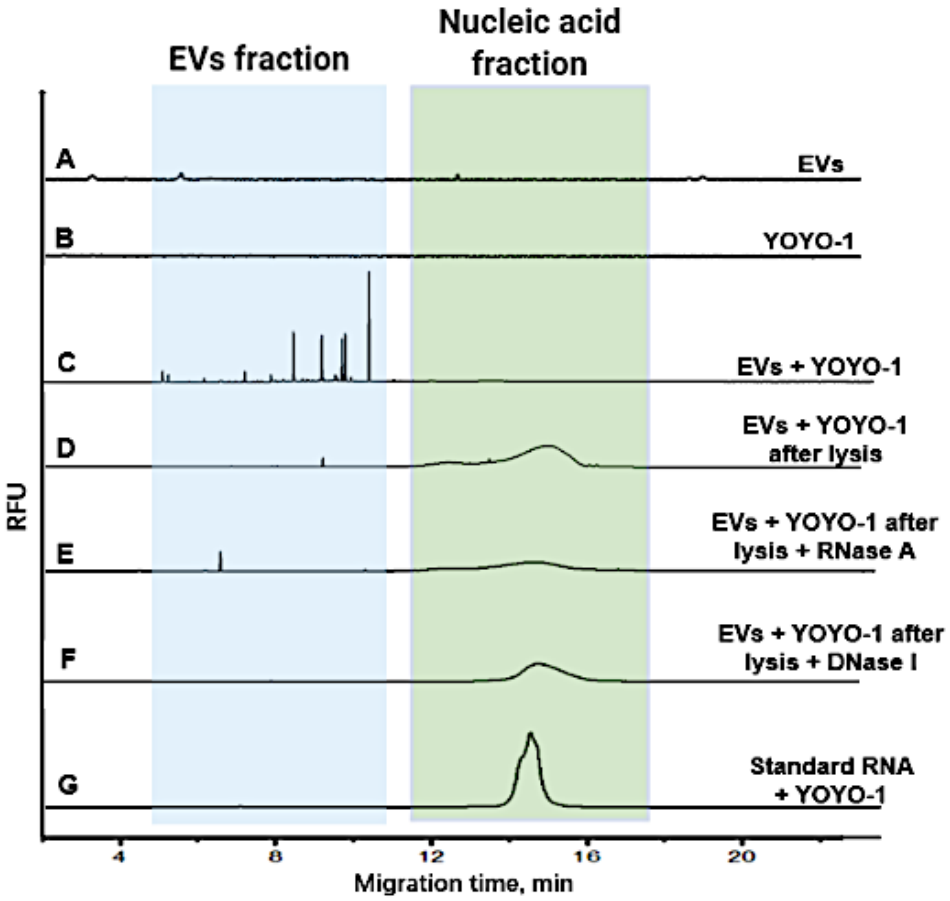

Figure 2.6 EVqCE electropherograms of EVs isolated from cancer cell lines. (A) Control experiment: EVs without YOYO-1 dye. (B) Control experiment: 2 μM YOYO-1 dye only. (C) EVs from the MDA-MB-231 cells were stained with YOYO-1 before lysis. (D) EVs from the MDA-MB-231 cells were lysed by 0.1% SDS and stained with YOYO-1. (E) After SDS lysis, RNase A was added to EVs to remove all free RNA from

the sample. (F) After SDS lysis, DNase I was added to the EVs to remove all free DNA. (G) yeast RNA (150 ng/mL) was stained with YOYO-1 only.

2.4.3 Quantitation of EVs isolated from cell lines with CZE

From the above results, it can be noted that CE cannot quantify EVs directly since the multiple spikes are irreproducible. However, it was thought that, to lyse the EVs and release the nucleic acids inside. Therefore, by determining the increase of DNA or RNA concentration, the average mass of DNA or RNA in each EV particle can be calculated. Thus, for any unknown EV sample, the developed method needs to do the quantification of EVs, which is obtained from the increasing amount of DNA or RNA after EV lysis and then divide it by the average mass of DNA or RNA in each particle.

To lyse EVs particles and release the nucleic acids, several surfactants were evaluated. Tween 20, Triton X-100 and sodium dodecyl sulphate (SDS) were prepared with samples at the proper concentration that has already shown the highest efficiency.[79] CE results finally showed that the EV sample treated with 0.1% (w/v) SDS for 30 min at room temperature could lyse most of the EV particles and has the highest lysis efficiency among the selected surfactants. This result also corroborates with the results in a published paper.[79]

Quantifying EVs could be divided into four steps. In the first step, the main idea was to find an increased concentration of RNA after lysis. As shown in **Figure 2.7 A**, the original EV sample exhibited a nucleic acid peak containing both DNA and RNA from isolation processes. RNase A was then added to the sample to eliminate the free RNA and to leave the free original DNA alone (**Figure 2.7 B**). However, in most instances, the nucleic acid peak is very small, which can be ignored. After the addition of SDS, multiple sharp peaks disappeared, and the wide peak increased its area. At this time, the wide nucleic acid peak contained RNA from EVs and DNA from both isolation and EVs (**Figure 2.7 C**). Any RNA released from EVs can be eliminated by the addition of RNase A again to leave only DNA in the sample (**Figure 2.7 D**).

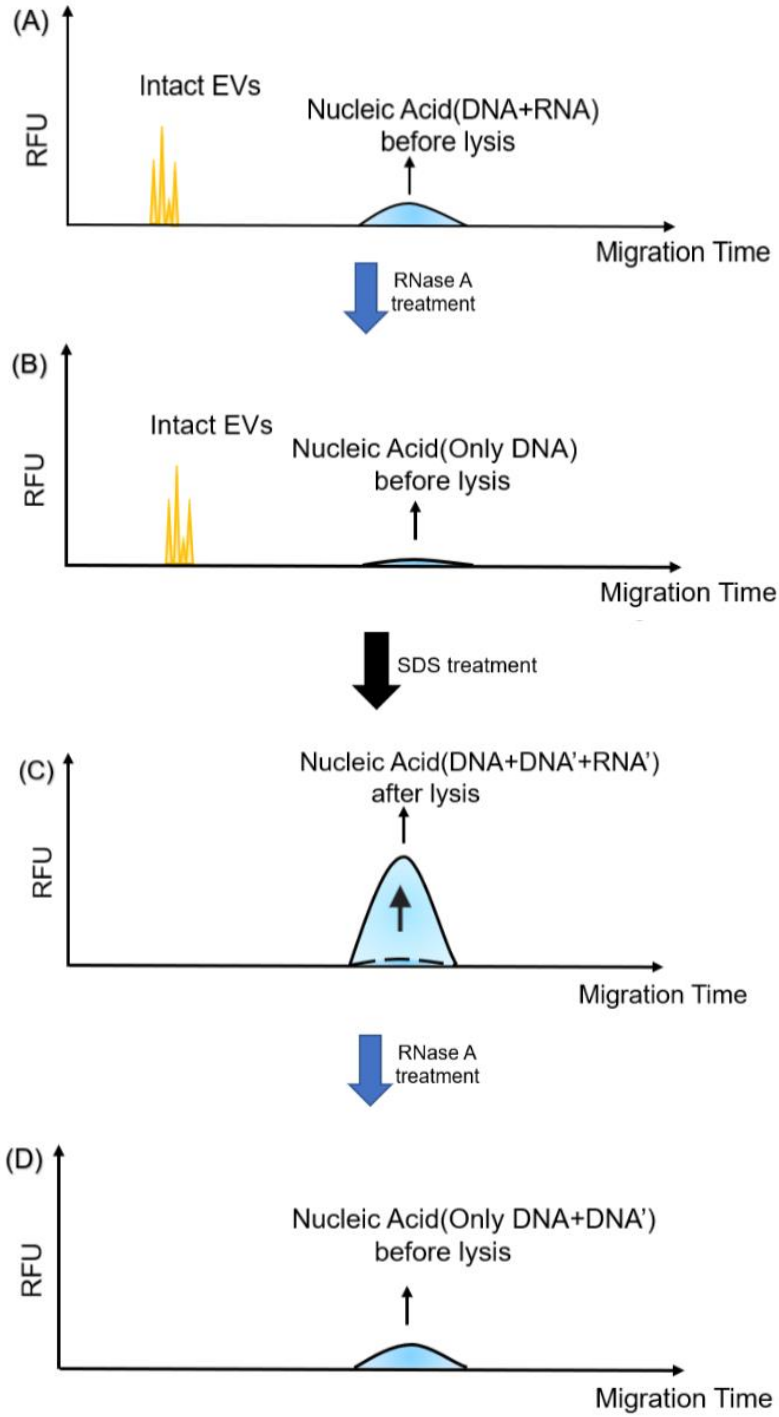

Figure 2.7 Schematic representation of first part in EV quantification. DNA and RNA in this figure represent the original DNA and RNA obtained from the EV isolation process. DNA' and RNA' represent the DNA and RNA released from EVs.

The decreased peak area represented the concentration of RNA from lysed EVs that could be determined from the RNA calibration curve. The RNA calibration curve was built by plotting fluorescent intensities of RNA standards stained with YOYO-1 as a function of their concentrations (**Figure 2.8**). The concentration of released RNA in one

unknown EV sample after lysis was acquired by calculating the decrease in peak area in the form of a relative fluorescence unit (RFU) and finding a concentration value in the curve. All the calculations and curve fitting were done using Origin 9.0 software.

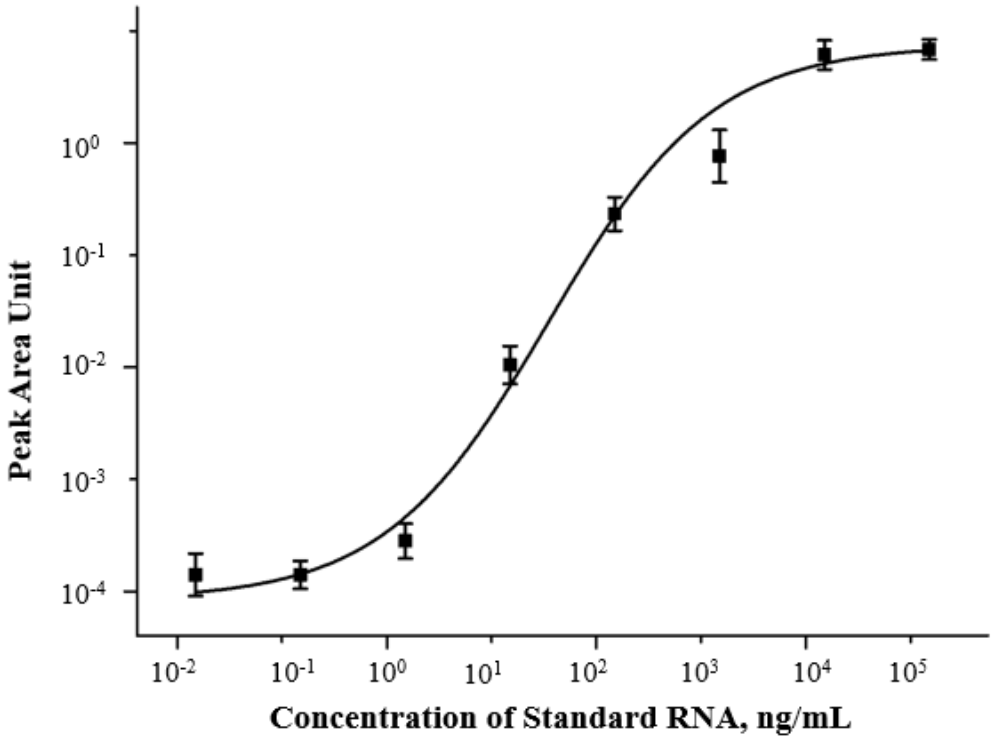

Figure 2.8 Calibration curve of YOYO-1 stained different concentrations of yeast RNA for finding the concentration of RNA released from EVs after lysis. 2 μM of YOYO-1 dye was used to stain the RNA. Error bars for each sample were obtained from three times repeating CE analysis in the same condition.

The fitting equation shows in equation 2.1:

$$y = -4.07 + \frac{4.94}{1+10^{(1.54-x)\cdot 0.56}} \quad (2.1)$$

where x is the concentration of standard RNA, and y is RFU.

The determination of a decrease in the concentration of intact EV particles was the second step, which was performed with the help of flow cytometry. By running the Apogee beads with similar size to EVs for 120 seconds, the average injection speed $\bar{v}$ (mL/min) can be measured, which is regarded as the average speed $\bar{v}$ of EVs. According to the result, 71555 particles were detected after 120 seconds; the final speed of beads flow was 4.125×10^{-3} μL/s. Therefore, the concentration of EV particles in the sample, [*EV*], can be calculated by the total number of EV particles N_c passing through

the detector in a certain range of time t with a certain speed $\bar{v}$:

$$[EV] = \frac{N_c}{\bar{v}t} \tag{2.2}$$

The EV samples before and after lysis were all stained with YOYO-1 and FM 5-95 for flow cytometry experiments (**Figure 2.9**). FM 5-95 is able to stain the lipid membrane, and YOYO-1 could stain nucleic acids; the particles showed "double-positive" results, which means those labelled with two dyes were intact EVs. SDS as a detergent could destroy the membranes of EVs, causing the number of particles with "double-positive" to decrease. The concentration of EVs before and after lysis could be denoted as $[EV]_{\text{before}}$ and $[EV]_{\text{after}}$, and they can be calculated from equation 2.2. Thus, the decrement of EV concentration after lysis $\Delta[EV]$ can be calculated:

$$\Delta[EV] = [EV]_{\text{before}} - [EV]_{\text{after}} \tag{2.3}$$

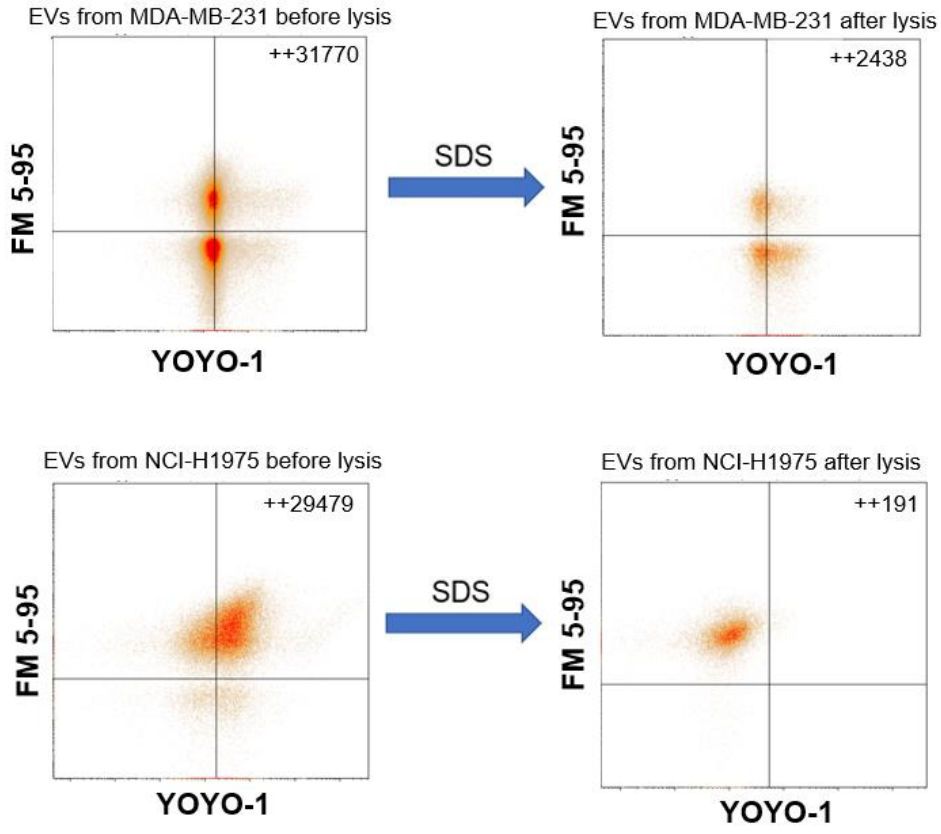

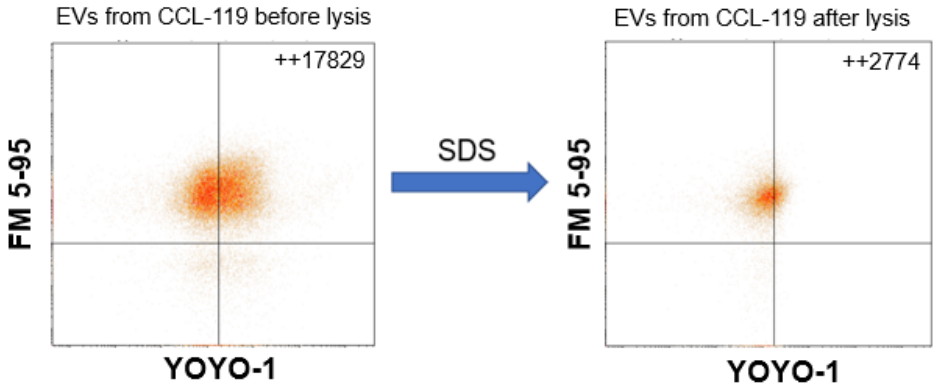

Figure 2.9 The results of flow cytometry with three cell lines to calculate the decrement of EV concentration after lysis. EVs were stained by FM 5-95 and YOYO-1 before and after SDS treatment. The number of events in the double-positive area is written in the top-right corner. An unstained sample was used to set the gate.

In the third step, the average mass of RNA in each intact EV particle ($\bar{m}_{RNA}$) is calculated. The concentration of RNA released from intact EVs after lysis can be measured from CE data combined with the RNA calibration curve, while the decrement of EV concentration after lysis can be measured from flow cytometry data. $\bar{m}_{RNA}$ could be calculated by the equation 2.4:

$$\bar{m}_{RNA} = \frac{\Delta[RNA](10^{-9})}{\Delta[EV]} \tag{2.4}$$

where $\Delta[RNA]$ is the concentration of RNA from intact EV particles.

Several samples were tested to verify this idea, and the final value of $\bar{m}_{RNA}$ for EVs from the MDA-MB-231 cell line is $(1.96 \pm 0.3)\times10^{-13}$ g/particle, the $\bar{m}_{RNA}$ values for NCI-H1975 and CCL-119 cell lines are $(3.75 \pm 0.4)\times10^{-13}$ g/particle and $(3.33 \pm 0.2)\times10^{-13}$ g/particle, respectively. These results agreed with the conclusion that a typical mammalian cell contains 2×10^{-11} g of total RNA.[80]

The last step of the EV quantification is very simple. By rearranging equation 2.4, for any unknown EV samples from the three cell lines, the concentration of intact EVs can be calculated from:

$$[EV]_{\text{unknown}} = \frac{\Delta[RNA](10^{-9})}{\bar{m}_{RNA}} \tag{2.5}$$

The only thing that needs to do to quantify an unknown EV sample is to obtain $\Delta[EV]$ by CE.

2.4.4 EVqCE compared with other quantification methods

The same EVs were also quantified by other methods to validate EVqCE. EVs from three cell lines with proper dilutions. NTA analysis would directly report the concentration of EVs. Flow cytometry was also able to quantify EVs by staining the samples with two antibodies, i.e., anti-human CD9 and anti-human CD63, measuring the number of particles in the "double-positive" area and calculating by equation 2.2. The concentrations of EVs from MDA-MB-231, NCI-H1975 and CCL-119 with these three different quantification methods were summarized in **Table 2.1**.

Table 2.1 The concentration of EVs isolated from three cell lines acquired by EVqCE, NTA and flow cytometry.

Quantification Method	MDA-MB-231	NCl-H1975	CCL-119
EVqCE (particles/mL)	$(5.1 \pm 0.2) \times 10^9$	$(1.4 \pm 0.1) \times 10^9$	$(1.3 \pm 0.4) \times 10^9$
NTA (particles/mL)	$(4.9 \pm 0.1) \times 10^{10}$	$(2.3 \pm 0.2) \times 10^{10}$	$(2.6 \pm 0.3) \times 10^{10}$
Flow cytometry (particles/mL)	$(1.7 \pm 0.3) \times 10^9$	$(3.6 \pm 0.7) \times 10^8$	$(6.0 \pm 0.8) \times 10^8$

It is clear that NTA results have the highest concentration of EVs among the three methods, as it counts all particles, not only EVs. Flow cytometry shows a lower concentration since antibodies are just able to recognize a part of a subpopulation of EVs, and it is not sensitive for small particle detection. The EV concentrations gained from EVqCE are in the range between NTA and flow cytometry, thus showing the reliable and reproducible results obtained by the EVqCE method.

2.5 Conclusion

In this chapter, I demonstrated a new method to quantify intact EVs from three different cancer cell lines by using EVqCE. The CE with LIF detector is very sensitive and accurate, and the experiment can be done within one hour and require minimal skills for the optimization of CE separation. It also requires a small volume of samples, and the cost of analysis is very low. The most important advantage is that it does not require any pre-treatment for EVs to be detected. Although EV samples possess lots of

impurities, EVqCE is able to focus on EVs and free nucleic acids with the addition of YOYO-1 dye. The results from EVqCE compare well with the results from NTA and flow cytometry, indicating the reliability of this new method.

Chapter 3: Salivary Extracellular Vesicle Quantitative Capillary Electrophoresis (Salivary EVqCE)

3.1 Objectives and contributions

In chapter 2, the new technique EVqCE was developed successfully to quantify EV samples isolated from three different cancer cell lines. Getting encouragement from the results obtained from EVqCE, I thought of enacting this method for the quantification of EVs from human saliva. This chapter is aiming to modify EVqCE and its implementation towards the detection of EVs isolated from human saliva.

All the flow cytometry experiments were performed under the guidance of Dr. Shahrokh Ghobadloo. TEM was operated by Dr. Yun Liu. I performed all the optimization of EVs isolation from saliva and responsible for performing CE experiments.

3.2 Introduction

Oral cancer accounts for 1-2% of all types of cancer worldwide in which oral squamous cell carcinoma (OSCC) is the most frequent type amongst patients.[81] This disease exercises a great influence on different sites in the oral cavity, including the tongue, floor of the mouth, and cheeks.[82] Oral cancer is hard to diagnose at an early stage currently, which causes half of the patients with oral cancer to only have a 20% survival rate after being confirmed.[81, 83] Previous studies have already indicated that saliva has the potential of monitoring health by the proteomic analysis.[84] Moreover, recent studies have shown that the molecules delivered by salivary EVs participate in important intracellular signalling mechanisms, and the number of released salivary EV from healthy individuals and cancer patients is different.[85, 86] Therefore, studying the

average mass of RNA in each salivary EV and finding a method to quantify EVs from saliva quickly are meaningful, which may provide more information for future study.

It is known that EVs involve the whole body and can be easily separated from all body fluids (such as blood, saliva, urine, breast milk, cerebrospinal fluids). To understand their biological roles and to extend their functions in clinical applications, human saliva, which is non-invasive and easy to collect, has been increasingly used for research to reveal the differences between a healthy cell and a cancer cell.

Nowadays, most of the quantification methods require pre-treatments to increase the purity of EV samples.[87, 88] Henceforth, developing a simple and cost-effective method for the quantification of EVs is quite necessary.

In this chapter, salivary EVqCE was used to quantify EVs isolated from human saliva. This approach has slight changes from EVqCE due to the specificity of saliva samples. By comparing with the quantification results from other methods, salivary EVqCE proved that it could be considered as a cheap, fast quantitative method with reproducible results for many applications in the biomedical field.

3.3 Materials and methods

3.3.1 Chemicals and materials

The following chemicals were purchased: sodium dodecyl sulphate (cat. no. BP166-500, Fisher Scientific, China), RNase A (cat. no. 21210, Affymetrix, U.S.A.), yeast ribonucleic acid (cat. no. 55714, Calbiochem, U.S.A.), YOYO-1 Iodide (cat. no. N7565, Invitrogen, U.S.A.), Dulbecco's phosphate-buffered saline (cat. no. D8537, Sigma, U.K.), sodium borate decahydrate (cat. no. SX0355-1, EMD Chemicals, U.S.A.), fluorescein (cat. no. F2456, Sigma, U.S.A.), EDTA (cat. no. E9884, Sigma-Aldrich, U.S.A.), CFDA-SE (cat. no. V12883, Invitrogen, U.S.A.), anti-human CD63 APC, clone H5C6 (cat. no. S32703), FM 5-95 (cat. no. T23360), UranyLess (cat. no. 22409), starch from rice (cat. no. S7260, Sigma-Aldrich, U.S.A.). The bare silica capillary with o.d. 362.0 μm, and i.d. 75.3 μm (cat. no. TSP075375, Phoenix, AZ, U.S.A.) was used

for all CE experiments. The Synergy UV water purification system equipped with a 0.22 μm filter was performed to provide free nuclease ionized water for buffer preparation.

3.3.2 Salivary EV isolation and collection

Saliva samples were collected according to the certification of ethics approval (attached at the appendix) from healthy individuals (n=4) in the morning after brushing teeth. The healthy donors were also required not to eat before saliva collection because food residues might cause contamination of their samples. 20 mL saliva was stored in 50 mL tubes in 4°C refrigerator for further use.

For the isolation of EVs from human saliva, two different approaches were performed. The details of the procedures were depicted in **Figure 3.1**. Initially, the saliva was diluted with the same volume of filtered PBS, with proper shaking, followed by vortexing for a few seconds to make the saliva mixed completely. The sample was centrifuged with 300 g at 4 °C for 20 min to remove the food debris and cells. The supernatant was collected and centrifuged with 2,600 g for 20 min to remove the large proteins. From here, two different methods of isolation were followed. The first method was to centrifuge the supernatant directly with 100,000g at 4 °C for 3 h. The pellet was resuspended in 1 mL PBS and stored at 4 °C for further use. The second isolation method includes the treatment with starch (1 g of starch per 10 mL of saliva sample). Starch was added before ultracentrifugation. Then, the supernatant was thoroughly mixed with the starch for 30 min using a shaker. Following centrifugation at 2,600 g for 30 min starch would completely settle down, and the supernatant was collected. The supernatant was again subjected to 100,000g ultracentrifugation for 3 h, and the pellet was collected. The pellet was resuspended with 1 mL PBS and stored at 4 °C until further use.

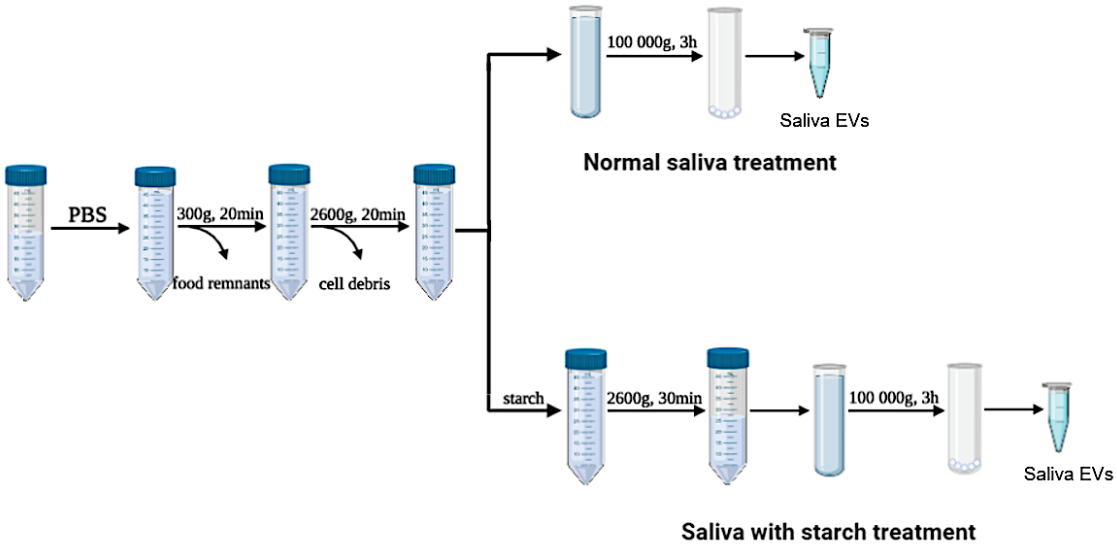

Figure 3.1 Schematic representation of two different isolation methods of EVs from saliva.

It should be noted that all the pellets after ultracentrifugation were viscous, and saliva samples collected from both isolation methods contained white “flocs” settled to the bottom after a few hours standing. Thereafter, transparent supernatant was collected for the following CE experiments.

3.3.3 Preparation of saliva EV samples and calibration curve

The EVs isolated from saliva are somehow similar to the EVs isolated from cancer cells concerning their structure and composition and hence can be detected by CE with YOYO-1 staining. For this, 1 μL of 2 μM YOYO-1 was incubated with 48 μL of samples or standard RNA at different concentrations. Intact saliva EVs particles were lysed by 0.1% (w/v) SDS. Besides, for saliva EVs, 1 μL of 500 nM fluorescein was added as an internal standard.

Standard RNA solutions with a concentration of 0.02, 0.04, 0.06, 0.08, 0.10 or 0.12 ng/mL were stained with YOYO-1 and analyzed by CE instrument to build an RNA calibration curve for this experiment.

3.3.4 TEM for saliva EVs

The same materials and staining dye used for the saliva EV TEM experiment was used for TEM images of EVs from cell culture. The sample preparation for the procedure was the same as chapter 2.3.5. Dr. Yun Liu offered technical support.

3.3.5 NTA for saliva EVs

Saliva EVs were diluted with PBS before the NTA experiment. The same NTA instrument and parameters were used for saliva EVs analysis, as described in chapter 2.3.6. The instrument was also calibrated with polystyrene beads before experiments.

3.3.6 Flow cytometry for saliva EVs

The characterization of saliva EVs was performed using MoFlo Astrios EQ Cell Sorter. The dye CFDA-SE and the antibodies, i.e., anti-human CD63 APC, were utilized to identify the saliva EVs. The dye and antibodies were incubated with saliva EVs for 20 min in the dark.

The YOYO-1 and FM 5-95 were used for using salivary EVqCE to quantify saliva EVs. YOYO-1 stained EVs fraction was to keep the same condition as CE for calculation, whereas it can not only stain EVs containing nucleic acid but also stain free nucleic acids. Thus, FM 5-95 was used to help me only focus on EV vesicles. The sample preparation steps were already described in chapter 2.3.7. The unstained sample served as control. Sample preparation for the flow cytometry experiments was performed by me, and the operation of flow cytometry was carried out by Dr. Shahrokh Ghobadloo.

3.3.7 CE for saliva EVs

The procedures of all the CE experiments for saliva EVs were just the same as that for EVs from cell cultures. More details have been described in chapter 2.3.8.

3.3.8 Heating treatment for saliva EVs

Heating treatment was required after the addition of SDS. Saliva samples were put in small PCR tubes and heated at 95 °C for 30 min in a Mastercycle pro PCR System (Eppendorf, Canada).

3.4 Results and discussion

3.4.1 Saliva EVs characterization

NTA. NTA was utilized to estimate the size distribution and total concentration of saliva EVs. The result of the size distribution of saliva EVs was shown in **Figure 3.2**, where most of the particles were detected by NTA in the range of 100 to 300 nm. It was found that the most abundant particles are with a size of around 153.5 nm. The concentration of saliva EVs is 9.5×10^{11} particles/mL. The details of the results were demonstrated in **Table 3.2** with the saliva EV concentrations collected from the flow cytometry and salivary EVqCE. The results indicated that the concentration of saliva EVs from NTA is much higher than the concentrations obtained from the other two methods due to the non-specificity.

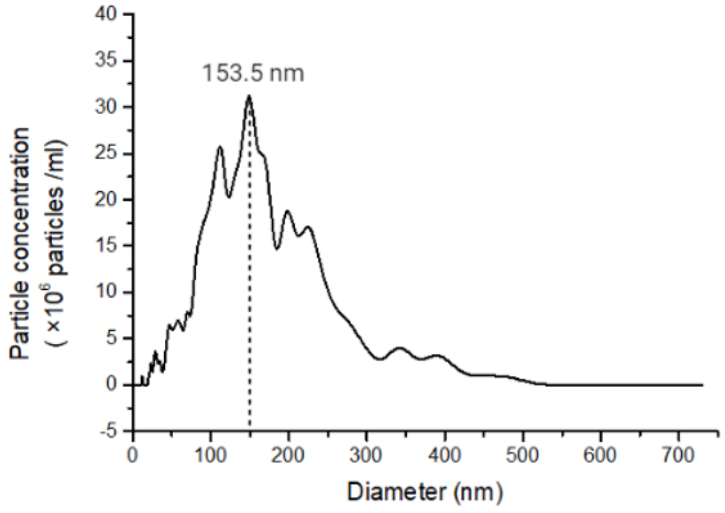

Figure 3.2 The results of nanoparticle tracking analysis of saliva EVs. The size distribution of EVs is derived from healthy human saliva. The size of the most abundant particles in the sample is depicted with the dotted line.

TEM. Saliva EV samples were stained by UranyLess. TEM could visualize different regions on the grid to capture the images of saliva EVs. The results were presented in **Figure 3.3**, showing the round vesicle with a double-layer membrane has a size of around 100 nm.

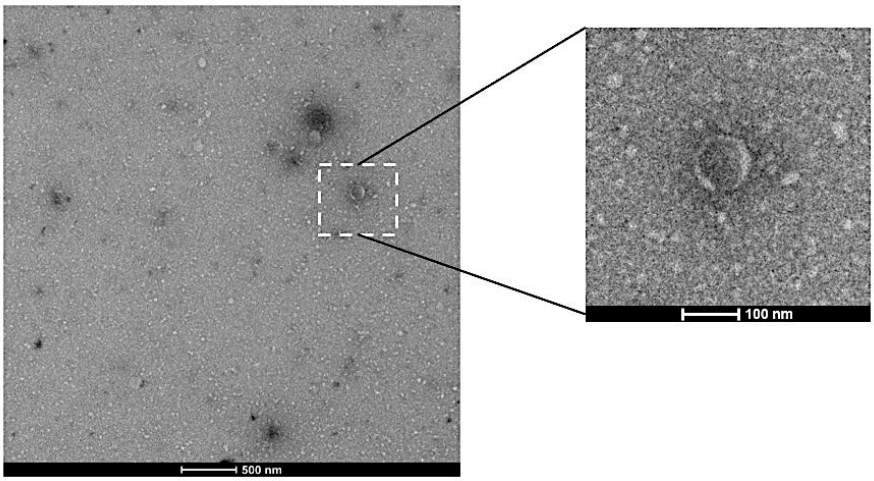

Figure 3.3 The TEM result of saliva EVs. Saliva EV samples were stained by UranyLess for 1 min.

Flow cytometry. For the flow cytometry characterization, CFDA-SE and anti-human CD 63 APC were incubated with EVs. CFDA-SE is highly cell-permeable due to its acetate groups. However, it is non-fluorescent unless it enters cells. The intracellular esterases remove the acetate groups, converting the molecule to the fluorescent ester. In this way, CFDA-SE could be considered as a dye that can characterize alive vesicles with an intact membrane. Anti-human CD63 APC could bind to the vesicles containing CD63 on their surface. In this way, the stained vesicles, which showed a double positive, could be considered as salivary EVs. The flow cytometry data of salivary EVs shown in **Figure 3.4**, demonstrate that the percentage of EVs in the sample to be 45.54%.

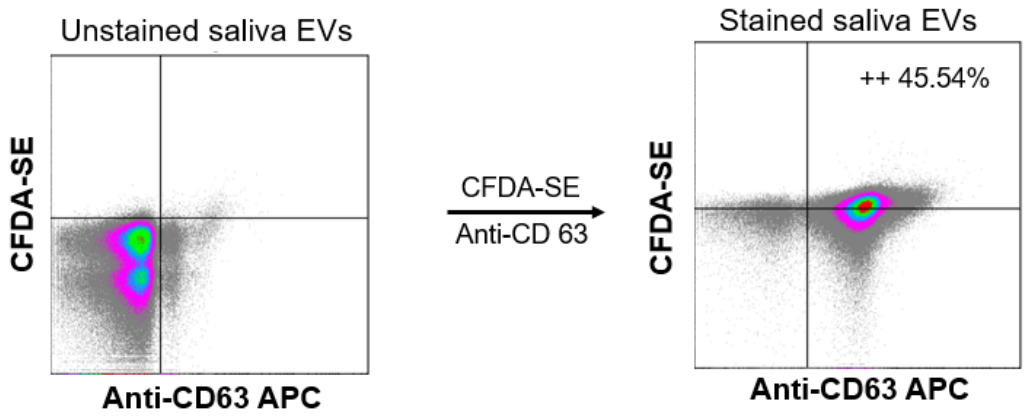

Figure 3.4 The results of the flow cytometry for saliva EVs characterization. Saliva EV samples were stained by CFDA-SE and anti-CD63 APC. The percentage (%) of events in the double-positive area was 45.54.

3.4.2 CE quantification for EVs isolated from saliva

For saliva EVs, all the conditions of the CE instrument are the same as EVqCE described in chapter 2.3.8. From our previous studies, EVqCE relies on the differential mobility of negatively charged free nucleic acids and intact EV particles. The principle of Salivary EVqCE is the same. The saliva sample containing intact saliva EV vesicles, free nucleic acids and impurities were stained with YOYO-1 fluorescent dye and injected into the capillary. Saliva EVs and nucleic acids are separated in capillary under the electric fields. EVs travelled faster compared with nucleic acids in the buffer solution, and thus, its earlier migration time can be visualized in the electropherogram.

However, one of the obstacles for saliva EVs detection is the interference of abundant amylase and other viscous proteins in saliva.[87] It can be mentioned here that the i.d. of capillary used for CE experiments is only 75.3 μm. The normal ultracentrifugation method for EVs isolation from saliva, which does not have any pre-treatment, leads to the attachment of viscous proteins to the interior wall of the capillary, affecting the velocity of EOF, blocking the capillary and reducing the reproducibility of results. To avoid the effect of these interfering proteins, starch was used to isolate the EVs from the saliva. Starch is an easily available and economical material that has been previously

used to remove amylase from saliva specifically based on their affinity interactions.[88] Thus, two isolation methods were tested and compared by using CE. Both saliva EVs samples collected by only ultracentrifugation and ultracentrifugation with starch pre-treatment were stained with YOYO-1 and run by CE (**Figure 3.5**, blue and green regions). The electropherograms of both EVs showed the same pattern, which contains multiple sharp peaks and a wide peak, but the electropherogram of salivary EVs with starch treatment showed a lower concentration of EVs fraction but did not influence their detection by CE. This situation is acceptable since I much more prefer to have a less sticky sample for CE.

Nevertheless, starch cannot eliminate all viscous proteins. This remaining problem still causes all peaks delay, which makes it hard to compare the results directly. To solve this problem, an internal standard (IS), fluorescein, was added in all saliva samples (**Figure 3.5**, red region). Fluorescein is very stable, and it does not interact with either EVs or nucleic acids. The addition of an internal standard makes it easier to compare all CE results of salivary EVs and decreases the bad effect of proteins. Based on that, further study was performed from salivary EVs samples treated with starch.

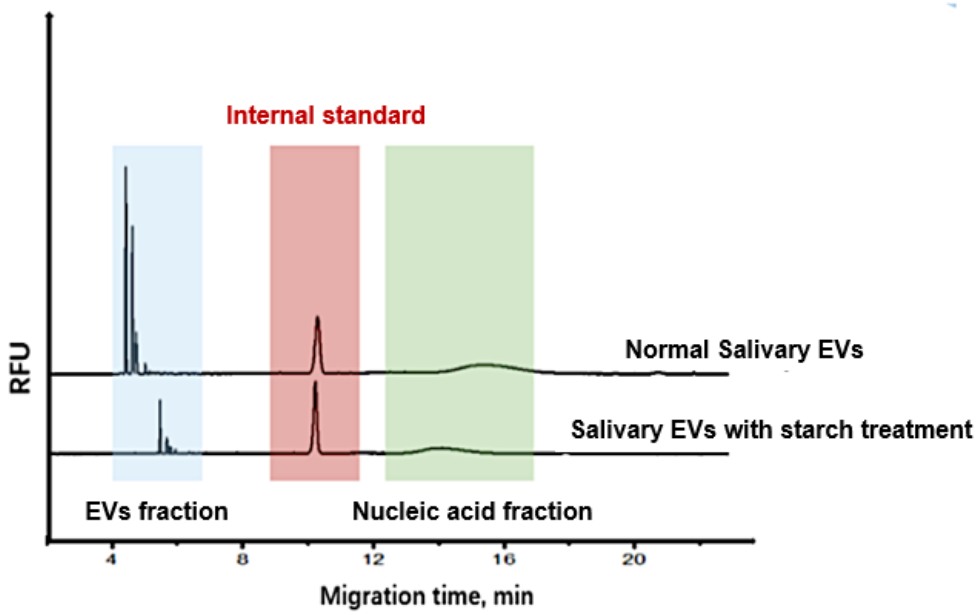

Figure 3.5 The CE results of saliva EV samples with and without starch treatment. Fluorescein as an internal standard was added in samples before running CE.

3.4.3 Eliminate the influence of RNase

Before starting to quantify saliva EVs, another existing challenge must be solved. It was ribonuclease (RNase). RNase plays an essential role in nucleic acid metabolism and can be found in every cell type. The human body fluids like urine, tears and saliva contain an abundance of RNase to defend against invading microorganisms.[89] This is also confirmed by our CE results (**Figure 3.6**). Saliva EV sample and 0.1 μg/mL standard RNA were stained with YOYO-1 separately, and then two of them mixed together also were incubated with dye; all of them were analyzed by CE. From a comparison of the results, the nucleic acid peak of saliva EVs mixed with standard RNA decreased dramatically. The peak areas of nucleic acid fraction in the three samples were also calculated by Origin software. A_1 represents the peak area of standard RNA, and it is 0.2787. A_2 is 0.0742, representing the peak area of free nucleic acid from the saliva EV sample. After running the mixture of saliva EVs and yeast RNA, the peak area of the nucleic acid fraction becomes 0.1206 (A_3). This is the clear evidence of the existence of RNase in saliva. Like EVqCE, if we want to quantify saliva EVs, the average mass of RNA contained in each saliva EV vesicle should be calculated first. While if the sample contains RNase, it will interact with RNA released from intact saliva EVs after lysis, inducing a lower mass of RNA. As a consequence, how to eliminate the influence of the existing RNase was the difficulty I needed to overcome before saliva EVs quantification.

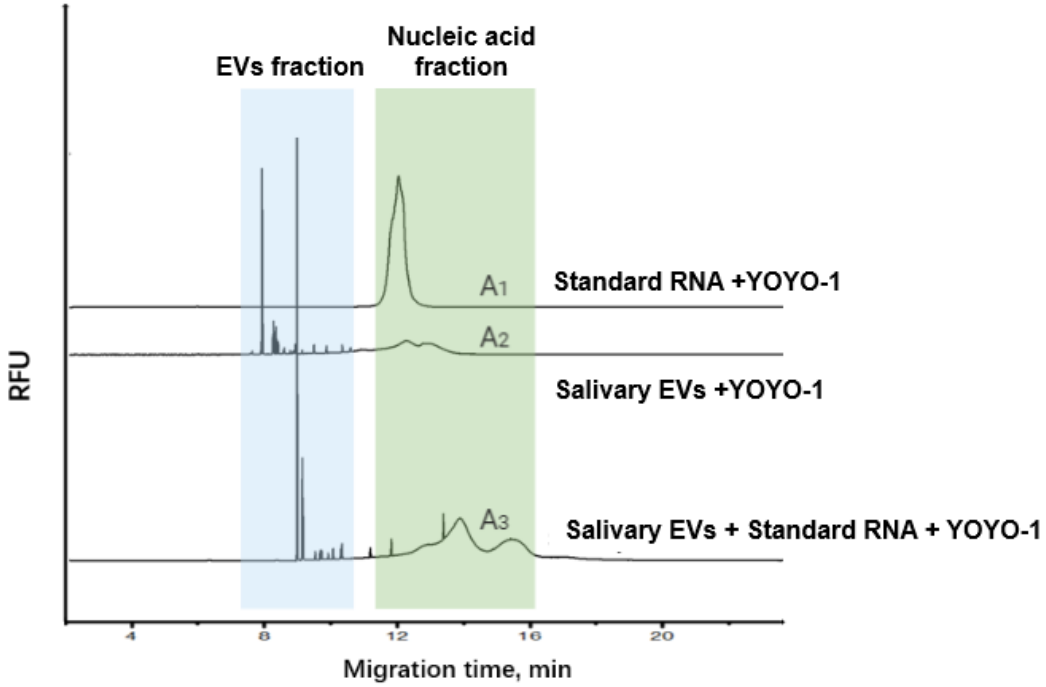

Figure 3.6 Confirmation of the presence of RNase in saliva EV samples using CE. 0.1 μg/mL yeast RNA was used as a standard RNA. Yeast RNA and saliva EV samples were run separately, and the mixture of yeast RNA and saliva EVs was also run by CE. A_1, A_2 and A_3 represent the peak area of nucleic acid fraction in three runs.

As the previous studies have shown, EDTA is a metal chelator that is used to inactivate nucleases.[89, 90] Thus, I tried to use EDTA to saliva EVs samples to inhibit RNase. But due to some unknown reasons, EDTA did not show significant results in saliva samples, and results were abnormal compared to EVqCE results.

Heating enables to not only help lyse saliva EVs but also denature proteins by disrupting hydrogen bonds within proteins and hydrophobic interactions between proteins. Therefore, for the salivary EVqCE method, the 0.1% (w/v) of SDS combined with heating was used to lyse saliva EVs completely and eliminate the effect of the original RNase. Complete lysis of saliva EVs was confirmed by the disappearance of spike peaks, which represent the saliva EVs fraction, and after SDS treatment and heating, the increase showed in the nucleic acid peak. However, the sequence of SDS addition and heating treatment can produce different results. The same saliva EVs sample was separated into four samples to determine which addition sequence has the highest efficiency of lysis and lowest influence of original RNase: (1) saliva EVs with

starch treatment sample was first heated to 95 ℃ for 30 min, then incubated with SDS for 30 min and stained with YOYO-1 dye; (2) saliva EVs with starch treatment sample was first stained with YOYO-1 dye, heated at 95 ℃ for 30 min and used SDS to lysis; (3) saliva EVs with starch treatment sample was first added SDS, heating, and with the addition of YOYO-1; (4) saliva EVs with starch treatment sample was treated with SDS, added YOYO-1 dye next and then heating (**Figure 3.7**). Four samples with different addition sequences were run five times continuously with CE. Each run took 40 min to finish. The aim of this step was to verify whether, with the increased time, the peak area of nucleic acid decreased or not. The results, without any decrement of peak area, suggested that the complete elimination of RNase in saliva EV samples. By comparing the four peak areas of nucleic acid, sample 3 was considered as the best addition sequence for all subsequent analysis (**Table 3.1**). Therefore, all saliva EVs were lysed by following the addition order of sample 3; the resulting nucleic acid peak contains DNA from isolation processes and RNA released from saliva EVs.

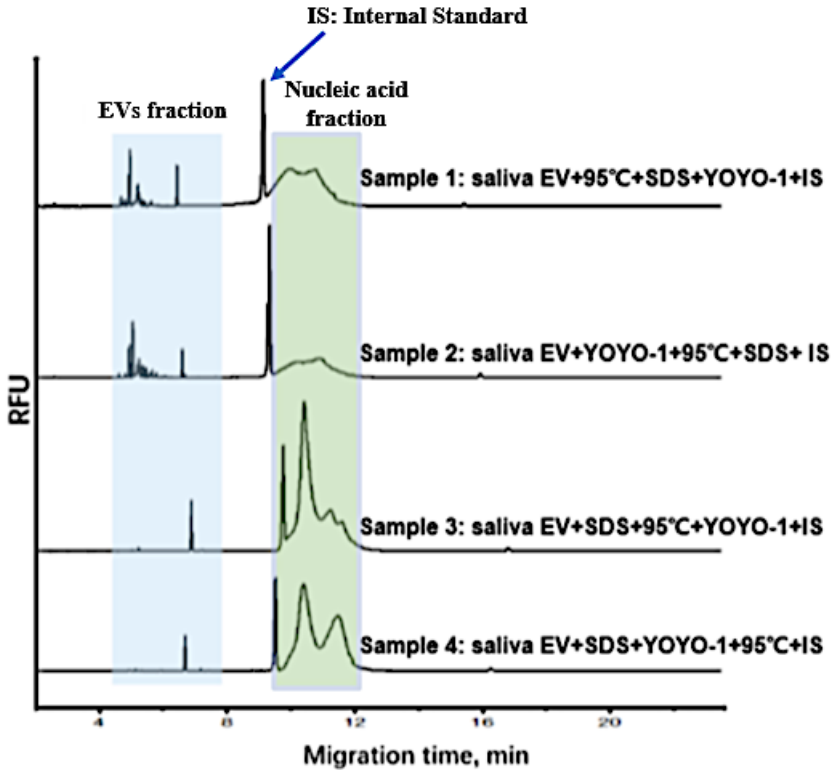

Figure 3.7 Saliva EVs were separated into four samples for different addition sequences. All the samples were added with internal standard and stained with YOYO-1 dye.

Table 3.1 The peak area of nucleic acids of four samples of saliva EVs.[a]

Time run by CE	Sample 1	Sample 2	Sample 3	Sample 4
1	0.2021	0.1089	0.3232	0.2711
2	0.2117	0.0894	0.3310	0.2848
3	0.2181	0.0971	0.3202	0.2807
4	0.2116	0.1020	0.3217	0.2865
5	0.2117	0.0933	0.3293	0.2732

[a] To check the reproducibility of the results, four samples were run five times by CE on the same day.

3.4.4 Quantification of saliva EVs

CE experiments were performed for the saliva EVs and YOYO-1 dye individually to prove that both of them did not have fluorescence. The internal standard was also used in CE. From the results shown in **Figure 3.8**, the peak of the internal standard does not overlap with the peak of nucleic acid. Saliva EVs samples before and after lysis were detected by CE, and the results show EVs fraction (Blue region), internal standard (Red region) and free nucleic acid (Green region). An intense decrease happened to nucleic acid peak after the addition of RNase, indicates that most nucleic acid contained in saliva EVs is RNA.

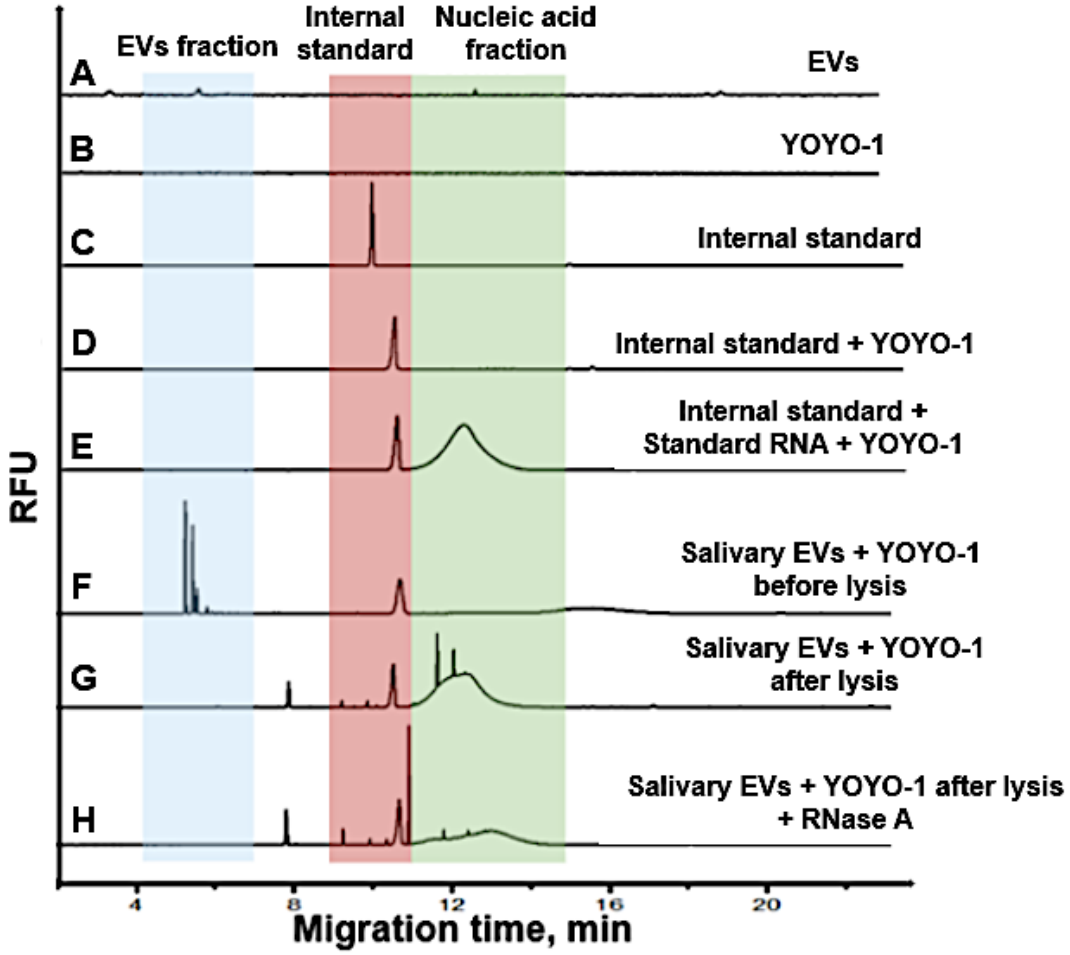

Figure 3.8 Experimental salivary EVqCE electropherograms of EVs from human saliva. (A) Control experiment: saliva EVs without YOYO-1 and internal standard. (B) Control experiment: YOYO-1 only. (C) Control experiment: internal standard only. (D) Control experiment: the internal standard was incubated with YOYO-1. (E) 0.1 μg/mL yeast RNA was stained by YOYO-1 with the addition of internal standard. (F) Saliva EVs are stained by YOYO-1 with the addition of internal standard before lysis. (G) Saliva EVs are stained by YOYO-1 with the addition of internal standard after lysis. (H) RNase was added to the saliva EV samples after lysis.

Four parts to quantify EVs from cell lines also apply to saliva EVs, named as salivary EVqCE. The goal of the first part is to calculate the RNA released from saliva EVs. Since the saliva EV samples already had RNase inside, I consider the free nucleic acid in the sample before lysis only possessed DNA. The total concentration of RNA from saliva EV vesicles can be determined by adding RNase inside after lysis and calculating it from a new standard RNA calibration curve (**Figure 3.9**). This time I built a new RNA calibration curve within a small concentration range to make it more accurate.

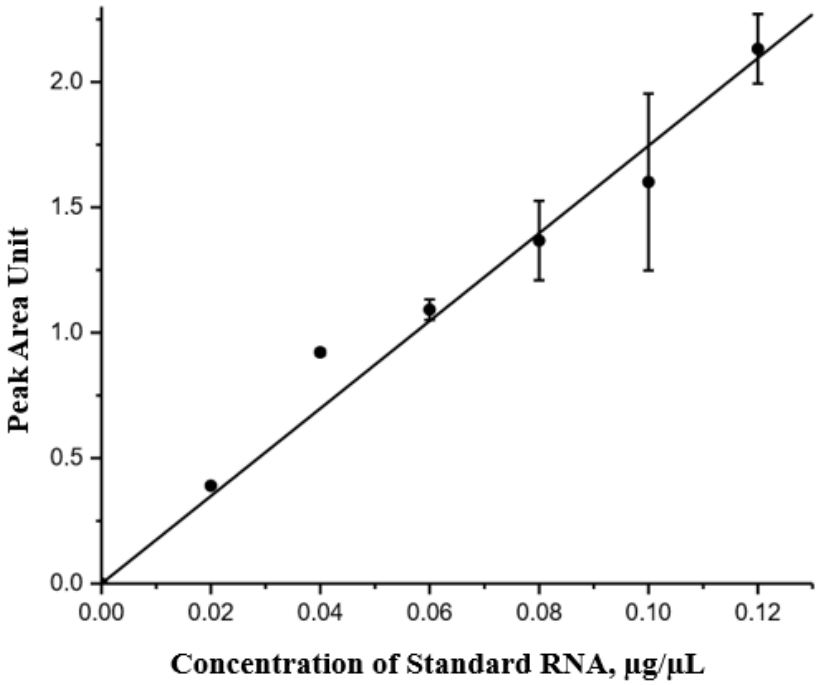

Figure 3.9 Calibration curve of YOYO-1 stained different concentrations of yeast RNA for saliva EV quantification. All the RNA samples were stained by YOYO-1. Error bars for each sample are obtained from three times repeating on CE in the same condition.

The fitting equation shows in equation 3.1:

$$y = 17.4593x + 0.0006 \quad (3.1)$$

In the second part, flow cytometry was used to calculate the decrement of the concentration of intact saliva EVs. The saliva samples with and without SDS lysis and heating treatment were incubated with FM 5-95 and anti-human CD63. Choose the particles in the double-positive area and then $[saliva\ EV]_{before}$ and $[saliva\ EV]_{after}$ can be calculated by using equation 2.2. $\Delta[EV]_{saliva}$ is therefore acquired from $[saliva\ EV]_{before}$ and $[saliva\ EV]_{after}$ by equation 2.3.

To calculate the average mass of RNA in each intact saliva EV particle ($\bar{m}_{saliva\ RNA}$) is the purpose of the third part. The majority of particles vanish after the addition of SDS and heat treatment (**Figure 3.10**). Since everything is the same as EVqCE, equation 2.4 could be used to calculate $\bar{m}_{saliva\ RNA}$. Three different saliva samples were tested by CE and flow cytometry to find the average of $\bar{m}_{saliva\ RNA}$, which is $(4.21 \pm 0.61) \times 10^{-13}$ g/particle.

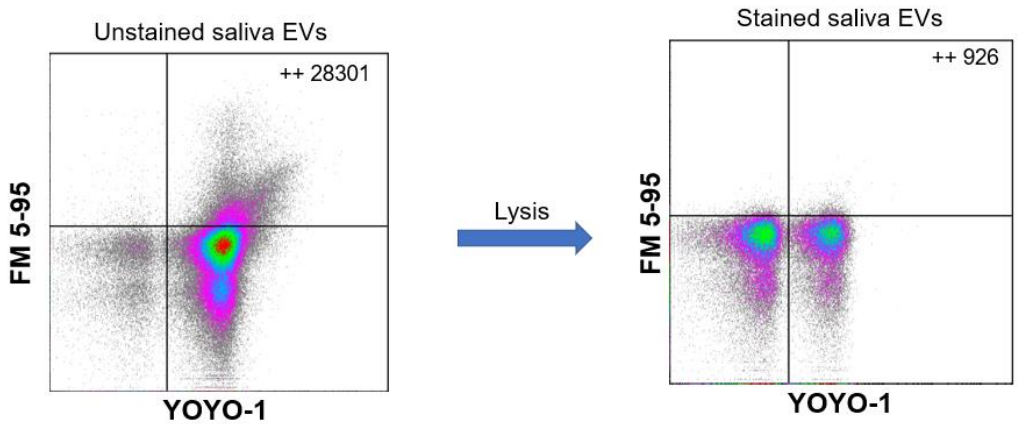

Figure 3.10 Flow cytometry results of saliva EVs before and after lysis. Saliva EVs were stained by YOYO-1 and FM 5-95. The number of events in the double-positive area is written in the top-right corner. The unstained sample was used to set the gate.

For the last part of quantification, I collected the other three unknown saliva EV samples, only run CE with these samples before and after lysis and to obtain the total concentration of RNA from the calibration curve. By using equation 2.5, the concentration of intact saliva EVs is calculated as a result of $(2.5 \pm 0.2) \times 10^9$ particles/mL.

These three unknown samples were also done by NTA and flow cytometry, and the results of all three methods are presented in **Table 3.2**. The experiments were performed three times, and the mean ± SD was presented. From this table, NTA has the highest concentration among the three methods as it can detect all particles in saliva samples, which still possess a lot of impurities. The flow cytometry and CE results have corroborated with each other.

Table 3.2 The concentration of saliva EVs acquired from salivary EVqCE, NTA and flow cytometry.

Quantification Method	**EVqCE (particles/mL)**	**NTA (particles/mL)**	**Flow cytometry (particles/mL)**
Salivary EVs (n=3)	$(2.5 \pm 0.2) \times 10^9$	$(9.6 \pm 0.2) \times 10^{11}$	$(3.2 \pm 0.1) \times 10^9$

3.5 Conclusion

In this chapter, salivary EVqCE was developed to quantify the EVs isolated from healthy human saliva. In order to solve the problem of high viscosity of saliva, starch was used for EVs isolation. The existence of RNase in saliva samples would interfere with saliva EVs quantification. After some attempts, heating treatment was performed, which is the most suitable way to eliminate the original RNase. The best optimization method of lysing of saliva EVs with SDS and heating was also demonstrated, which can not only remove RNase inside but also have a higher lysis efficiency. After that, the same ideas were applied to quantify saliva EVs. The results from salivary EVqCE also compared with those from NTA and flow cytometry (with CFDA-SE and anti-CD63), showing that saliva EVqCE is highly reproducible, and it can be utilized for future saliva EVs studies.

Chapter 4: Quality Control of Extracellular Vesicles

4.1 Objective

Studying EVs allows people to reveal the mechanism of diseases such as different types of cancer. However, the stability of the EVs for future studies and the degradation level under different conditions is unclear to researchers yet. In this chapter, EVqCE and salivary EVqCE were applied to study the quality control of EVs from cancer cell lines and human saliva, respectively.

4.2 Degradation analysis of EVs from the MDA-MB-231 cell line

4.2.1 Degradative conditions

EVs isolated from the MDA-MB-231 cell line were exposed to the following conditions to determine the degradation level of EVs. The conditions are *ultrasonic treatment*: 49 μL of EV samples were placed in a Branson Ultrasonic Cleaner (Model 3510, Branson Ultrasonics Corporation, USA) with 40 kHz power for 10 min at room temperature. *Extensive vortexing*: 49 μL of EV samples were continuously vortexed for 0.5 and 5 minutes at room temperature. *Freeze-thaw cycles*: 49 μL of EV samples were exposed to 10 freeze-thaw cycles. The cycles were performed by freezing EV samples at -80 °C for 1 min and then let them thaw at room temperature for around 1-2 min. *Storage*: EV samples were kept in 4 °C refrigerator for 7 and 14 days. All the samples were stained with 1 μL YOYO-1 before CE analysis.

4.2.2 Result and discussion

EVqCE could provide an easy way to investigate the level of EVs degradation without the need for quantification of the total amount of EV present in each sample. First, EV samples with and without SDS addition were run by CE, and data was analyzed to only gain the peak area of free nucleic acids A_1 and A_2 separately. Then EV samples in different degradative conditions were also run by CE, and peak areas were calculated as A'. To calculate the degradation level of EVs (%D) in varying conditions, equation 4.1 can be used:

$$\%D = \frac{A\prime - A_2}{A_1 - A_2} \cdot 100\% \qquad (4.1)$$

Here I considered that EV samples were lysed completely after adding SDS; all the nucleic acids from intact EVs were indicated as $A_1 - A_2$, EVs were degraded in different conditions, showing from the increased peak area of nucleic acid as A' $-A_2$. In this way, the degradation level could be calculated in percentage without more calculation processes.

The EV sample was degraded by 85.8 ± 25.8% after ultrasonic treatment for 10 min. 4.7 ± 1.8% and 12.5 ± 3.1% were the %D of samples with extensive vortexing for 0.5 and 5 min, respectively. After 10 freeze-thaw cycles, 40.3 ± 7.0% of EVs were degraded. EV samples after 7 and 14 days were tested to show 3.1 ± 0.9% and 32.4 ± 6.5% of %D, respectively. The CE results of samples in each case were presented in **Figure 4.1**.

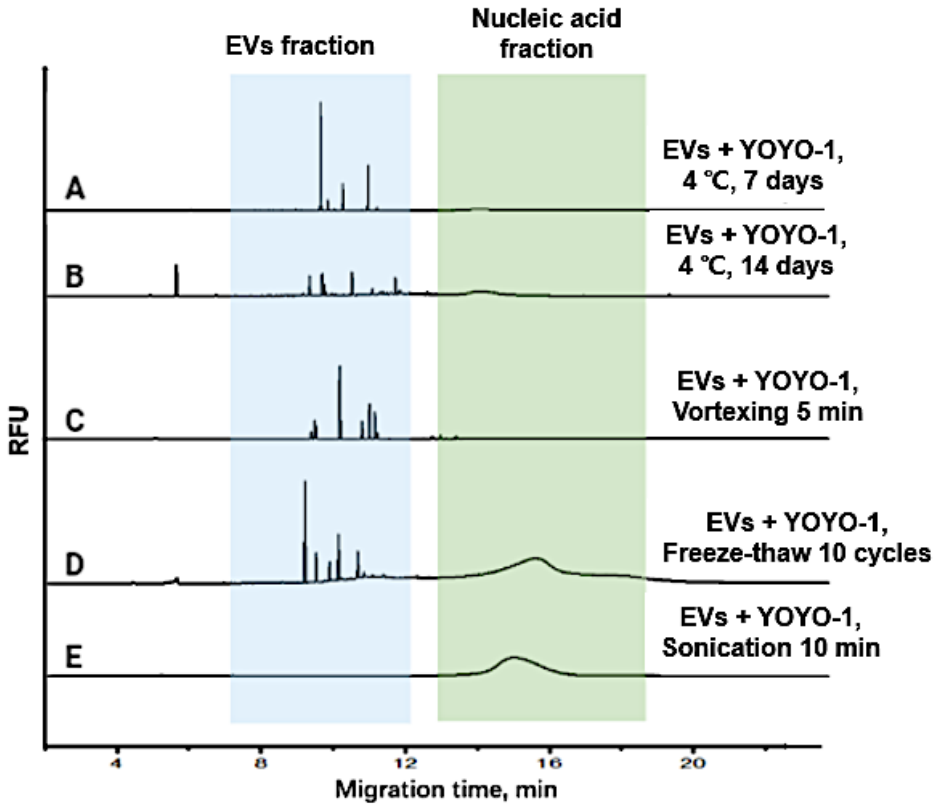

Figure 4.1 Experimental EVqCE electropherograms of the degradation of EVs from cell lines in different conditions. (A) EVs were tested after 7 days. (B) EVs were tested after 14 days. (C) EVs were tested after vortexing for 5 min. (D) EVs were tested after 10 freeze-thaw cycles. (E) EVs were tested after 10-min ultrasonication. All the EV samples were stained by YOYO-1.

It should be mentioned that samples with ultrasonic treatments had a higher degradation level, probably because sonication allowed the permeability in the lipid bilayer membrane of EVs, and then YOYO-1 dye is able to enter inside and bind to the nucleic acids. The result of the sample after freeze-thaw also indicates that some biological samples at very low temperatures are at risk of losing activity or degrading.

4.3 Degradation analysis of EVs from saliva

4.3.1 Degradative conditions

CE was also used to test saliva EVs exposed to several conditions to determine their degradation levels. The conditions are *ultrasonic treatment*: 48 µL of saliva EV samples

were ultrasonicated with 40 kHz power for 10 min at room temperature. *Extensive vortexing*: 48 μL of saliva EV samples were vortexed for 10 minutes at room temperature. *Freeze-thaw cycles*: 48 μL of saliva EV samples were exposed to 5 freeze-thaw cycles. *Storage*: EV samples were kept in 4 °C refrigerator for 10 and 30 days. All the samples were stained with 1 μL YOYO-1 and 1 μL internal standard (fluorescein) before CE detection.

4.3.2 Result and discussion

Due to the existence of an RNase in saliva samples, I cannot use the same equation to calculate the degradation level of saliva EV samples (saliva %D). However, there is another way to calculate saliva %D. I determined the presence of intact EV samples in different cases instead of calculating the increase of peak area of free nucleic acids. In other words, if I could find the survival rates of saliva EVs in different conditions, saliva %D could be calculated next.

Saliva samples before and after lysis were analyzed, and the peak area of nucleic acids was defined as A_b and A_a. Saliva EVs were degraded, and after that, samples were lysed again to obtain the peak area of nucleic acids from living and intact saliva EVs which was defined as A_c. By this means, saliva %D could be calculated from a new equation 4.2:

$$saliva\ \%D = (1 - \frac{A_c - A_b}{A_a - A_b}) \cdot 100\% \quad (4.2)$$

The CE result of saliva EVs in individual conditions is demonstrated in **Figure 4.2**. About 97.8 ± 1.4% of saliva EVs were degraded after 10-min ultrasonic treatment. The saliva %D was 63.3 ± 12.2% after freeze-thawing over 5 cycles. Vortexing for 10 min did have a degradation level of 46.6 ± 9.2%. While 26.6 ± 6.7% and 64.8 ± 7.6% of saliva EVs were degraded after 10 and 30 days.

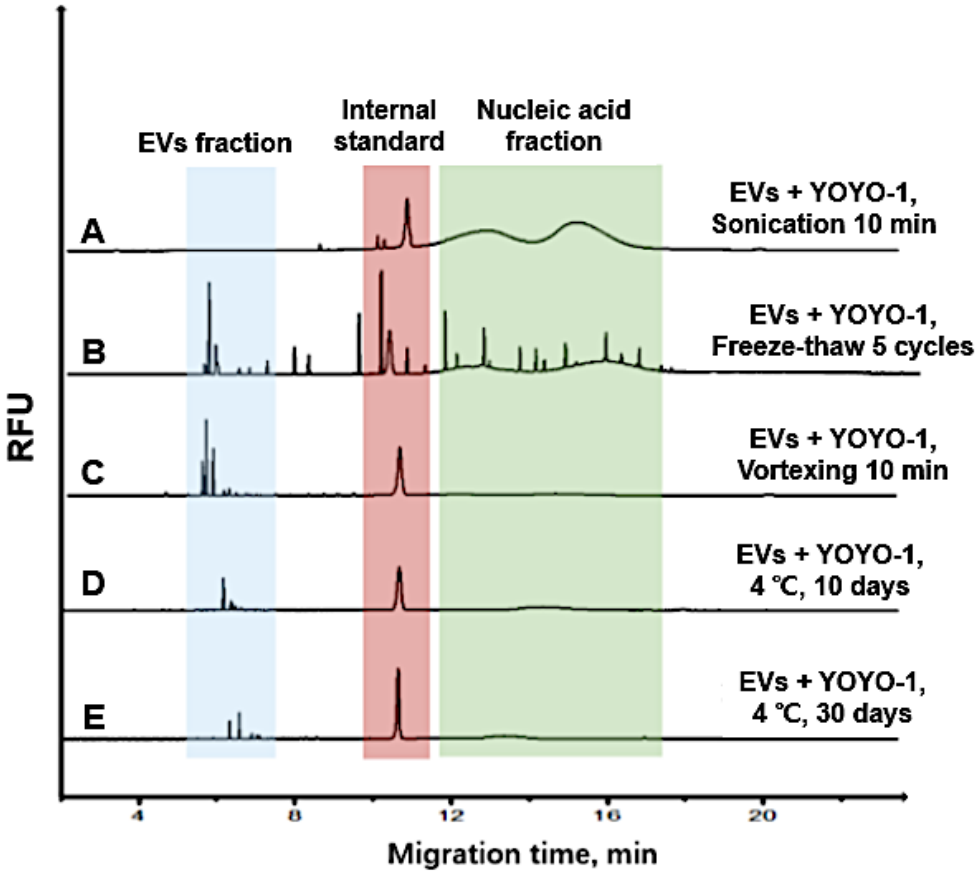

Figure 4.2 Experimental salivary EVqCE electropherograms of the degradation of saliva EVs in different conditions. (A) Saliva EVs with ultrasonic treatment for 10 min. (B) Saliva EVs with 5 cycles of freeze-thaw. (C) Saliva EVs with 10-min vortexing. (D) Saliva EVs were stored at 4 °C for 10 days. (E) Saliva EVs were stored at 4 °C for 30 days.

4.4 Conclusion

EVqCE and salivary EVqCE give the possibility of monitoring of EVs degradation, offering information about the sample stability under various conditions. We could predict that these methods are capable of being used as quality control of EVs from cell lines and saliva in future studies.

Chapter 6: Conclusion and Future Directions

Capillary electrophoresis is a well-established analytical technique used for separating ions. CE has already been applied in various analytical and bioanalytical fields, showing its universality and potentiality.[91-93] Extracellular vesicles have become a trending topic in recent years, and researchers want to uncover the specific role of EVs in diseases and cancers. Thus, to unravel the full potential of CE to quantify the EVs is the need of the hour.

EVqCE is a method developed for quantifying EVs from cancer cell lines by using a CE instrument with a LIF detector. The EVs samples were first characterized by NTA and flow cytometry, confirming its presence. These two methods could also estimate the concentration of EVs in unknown samples, which provide alternative results to compare with the results of EVqCE. EVqCE was divided into four steps to quantify EVs. After finding the average mass of RNA in each intact EV vesicle, the EV concentration of unknown samples could be obtained within one hour.

The second objective is to translate the EVqCE methods for the quantification of EVs in the body fluid, i.e., saliva. The process of EVs isolation from the human saliva was optimized, and starch was used to remove abundant amylase and viscous proteins to avoid blocking the capillary. Additionally, the original RNase was found in saliva samples, which could have an effect on saliva EV quantification. Heating treatment, combined with the addition of SDS, solved this problem greatly. The EVs lysis method was optimized, and the sequence of the process showed that almost all EVs were lysed with the elimination of RNase activity. Later, salivary EVqCE was applied to quantify saliva EVs, just like the way for EVs from cell lines.

Then, I extended the function of EVqCE to monitor the quality of EVs in different conditions without any sample quantification. The degradation level of EV samples under various conditions was calculated based on the peak area of nucleic acids present in the EVs.

In my studies, EVqCE and salivary EVqCE have shown its potential and reproducibility as compared with other known methods. These methods have high sensitivity, and they can quantify EV samples in a short time. The CE, as a widespread and commercial instrument, its simple operations and a small volume of sample requirements are attractive advantages. Last but not least, these methods could neglect impurities such as proteins and lipids in the samples, which do not require much time on sample pre-preparations.

Apart from this, it seems to be many potential applications of the EVqCE for different biological samples analysis. Here, I introduce not only this technology but also the idea which may be extended into other fields for sample quantification and real-time monitoring.

Appendix

24/09/2018

Université d'Ottawa
Bureau d'éthique et d'intégrité de la recherche

University of Ottawa
Office of Research Ethics and Integrity

CERTIFICAT D'APPROBATION ÉTHIQUE | CERTIFICATE OF ETHICS APPROVAL

Numéro du dossier / Ethics File Number	H-08-18-980
Titre du projet / Project Title	ANALYSIS OF HEALTHY HUMAN URINE AND SALIVA EXOSOMES FOR FUTURE DIAGNOSTIC APPLICATIONS
Type de projet / Project Type	Thèse de maîtrise / Master's thesis
Statut du projet / Project Status	Approuvé / Approved
Date d'approbation (jj/mm/aaaa) / Approval Date (dd/mm/yyyy)	24/09/2018
Date d'expiration (jj/mm/aaaa) / Expiry Date (dd/mm/yyyy)	23/09/2019

Équipe de recherche / Research Team

Chercheur / Researcher	Affiliation	Role
Vanessa SUSEVSKI	Département de chimie / Department of Chemistry	Chercheur Principal / Principal Investigator
Maxim BEREZOVSKI	Département de chimie / Department of Chemistry	Superviseur / Supervisor
Nico HÜTTMANN	Département de chimie / Department of Chemistry	Co-chercheur principal / Co-principal investigator
Emil ZARIPOV	Département de biologie / Department of Biology	Co-chercheur principal / Co-principal investigator
Yousef RISHA	Département de chimie / Department of Chemistry	Co-chercheur principal / Co-principal investigator
Prabir Kumar KULABHUSAN	Département de chimie / Department of Chemistry	Co-chercheur principal / Co-principal investigator
Suttinee POOLSUP		Co-chercheur / Co-investigator

Conditions spéciales ou commentaires / Special conditions or comments

550, rue Cumberland, pièce 154
Ottawa (Ontario) K1N 6N5 Canada

550 Cumberland Street, Room 154
Ottawa, Ontario K1N 6N5 Canada

Figure S1. Certification of ethics approval for analysis of healthy human urine and saliva exosomes for future diagnostic applications.

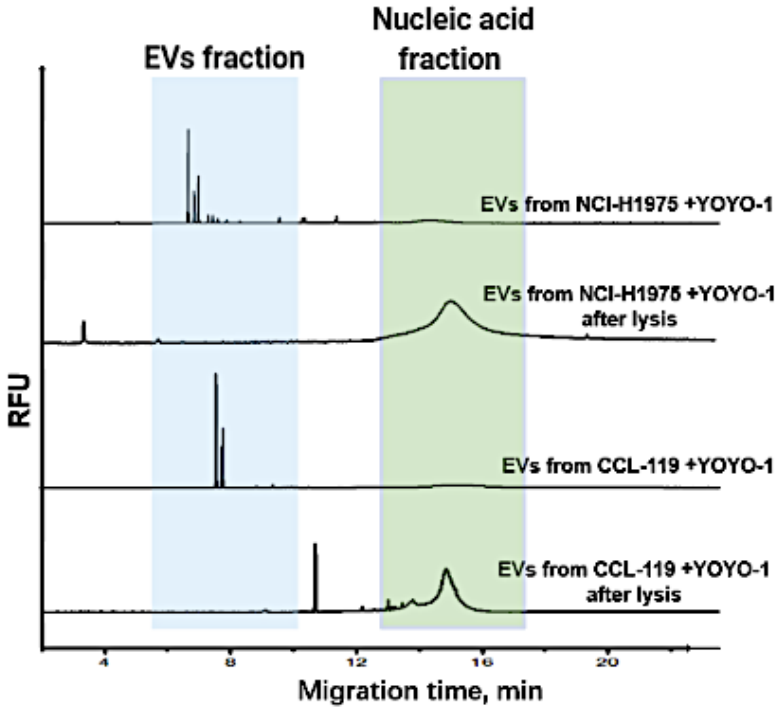

Figure S2. CE results of EVs from NCI-H1975 and CCL-119 cell lines. EV samples before and after lysis were stained with YOYO-1.

Reference

1. Hargett, Leslie A & Bauer, Natalie N On the origin of microparticles: From "platelet dust" to mediators of intercellular communication. *Pulmonary circulation* **3**, 329-340 (2013).
2. Wolf, Peter The nature and significance of platelet products in human plasma. *British journal of haematology* **13**, 269-288 (1967).
3. Sadallah, S, Eken, C *et al.* Ectosomes as modulators of inflammation and immunity. *Clinical Experimental Immunology* **163**, 26-32 (2011).
4. Wysoczynski, Marcin & Ratajczak, Mariusz Z Lung cancer secreted microvesicles: underappreciated modulators of microenvironment in expanding tumors. *International journal of cancer* **125**, 1595-1603 (2009).
5. Baj-Krzyworzeka, Monika, Majka, Marcin *et al.* Platelet-derived microparticles stimulate proliferation, survival, adhesion, and chemotaxis of hematopoietic cells. *Experimental hematology* **30**, 450-459 (2002).
6. Baj-Krzyworzeka, Monika, Szatanek, Rafał *et al.* Tumour-derived microvesicles modulate biological activity of human monocytes. *Immunology letters* **113**, 76-82 (2007).
7. Lee, Yi, El Andaloussi, Samir *et al.* Exosomes and microvesicles: extracellular vesicles for genetic information transfer and gene therapy. *Human molecular genetics* **21**, R125-R134 (2012).
8. Kesimer, Mehmet, Scull, Margaret *et al.* Characterization of exosome-like vesicles released from human tracheobronchial ciliated epithelium: a possible role in innate defense. *The FASEB Journal* **23**, 1858-1868 (2009).
9. Chaput, Nathalie & Théry, Clotilde in Seminars in immunopathology, Vol. 33 419-440 (Springer, 2011).
10. Khan, Mohsin, Nickoloff, Emily *et al.* Embryonic stem cell–derived exosomes promote endogenous repair mechanisms and enhance cardiac function following myocardial infarction. *Circulation research* **117**, 52-64 (2015).
11. Ratajczak, Janina, Miekus, K *et al.* Embryonic stem cell-derived microvesicles reprogram hematopoietic progenitors: evidence for horizontal transfer of mRNA and protein delivery. *Leukemia* **20**, 847-856 (2006).
12. Skog, Johan, Würdinger, Tom *et al.* Glioblastoma microvesicles transport RNA and proteins that promote tumour growth and provide diagnostic biomarkers. *Nature cell biology* **10**, 1470-1476 (2008).
13. Al-Nedawi, Khalid, Meehan, Brian *et al.* Intercellular transfer of the oncogenic receptor EGFRvIII by microvesicles derived from tumour cells. *Nature cell biology* **10**, 619-624 (2008).
14. Caby, Marie-Pierre, Lankar, Danielle *et al.* Exosomal-like vesicles are present in human blood plasma. *International immunology* **17**, 879-887 (2005).
15. Duijvesz, Diederick, Luider, Theo *et al.* Exosomes as biomarker treasure chests for prostate cancer. *uropean urology* **59**, 823-831 (2011).
16. Yang, Jieping, Wei, Fang *et al.* Detection of tumor cell-specific mRNA and protein in exosome-like microvesicles from blood and saliva. *PloS one* **9** (2014).

17. Chen, Walter W, Balaj, Leonora *et al.* BEAMing and droplet digital PCR analysis of mutant IDH1 mRNA in glioma patient serum and cerebrospinal fluid extracellular vesicles. *Molecular Therapy-Nucleic Acids* **2**, e109 (2013).
18. Théry, Clotilde, Witwer, Kenneth W *et al.* Minimal information for studies of extracellular vesicles 2018 (MISEV2018): a position statement of the International Society for Extracellular Vesicles and update of the MISEV2014 guidelines. *Journal of extracellular vesicles* **7**, 1535750 (2018).
19. Barrachina, Maria N, Calderón-Cruz, Beatriz *et al.* Application of extracellular vesicles proteomics to cardiovascular disease: guidelines, data analysis, and future perspectives. *Proteomics* **19**, 1800247 (2019).
20. Van der Pol, Edwin, Böing, Anita N *et al.* Classification, functions, and clinical relevance of extracellular vesicles. *Pharmacological reviews* **64**, 676-705 (2012).
21. Mathivanan, Suresh, Ji, Hong *et al.* Exosomes: extracellular organelles important in intercellular communication. *Journal of proteomics* **73**, 1907-1920 (2010).
22. Raposo, Graça & Stoorvogel, Willem Extracellular vesicles: exosomes, microvesicles, and friends. *Journal of Cell Biology* **200**, 373-383 (2013).
23. Kerr, John FR, Wyllie, Andrew H *et al.* Apoptosis: a basic biological phenomenon with wideranging implications in tissue kinetics. *British journal of cancer* **26**, 239-257 (1972).
24. Akers, Johnny C, Gonda, David *et al.* Biogenesis of extracellular vesicles (EV): exosomes, microvesicles, retrovirus-like vesicles, and apoptotic bodies. *Journal of neuro-oncology* **113**, 1-11 (2013).
25. Li, Irene & Nabet, Barzin Y Exosomes in the tumor microenvironment as mediators of cancer therapy resistance. *Molecular cancer* **18**, 32 (2019).
26. Selmaj, Igor, Mycko, Marcin P *et al.* The role of exosomes in CNS inflammation and their involvement in multiple sclerosis. *Journal of neuroimmunology* **306**, 1-10 (2017).
27. Lee, Jingyun, McKinney, Kimberly Q *et al.* Exosomal proteome analysis of cerebrospinal fluid detects biosignatures of neuromyelitis optica and multiple sclerosis. *Clinica Chimica Acta* **462**, 118-126 (2016).
28. Kanninen, Katja M, Bister, Nea *et al.* Exosomes as new diagnostic tools in CNS diseases. *Biochimica et Biophysica Acta -Molecular Basis of Disease* **1862**, 403-410 (2016).
29. Yuana, Yuana, Sturk, Auguste *et al.* Extracellular vesicles in physiological and pathological conditions. *Blood reviews* **27**, 31-39 (2013).
30. Friend, C, Marovitz, W *et al.* Observations on cell lines derived from a patient with Hodgkin's disease. *Cancer research* **38**, 2581-2591 (1978).
31. Bandu, Raju, Oh, Jae Won *et al.* Mass spectrometry-based proteome profiling of extracellular vesicles and their roles in cancer biology. *Experimental molecular medicine* **51**, 1-10 (2019).
32. Zhao, Hongyun, Achreja, Abhinav *et al.* The key role of extracellular vesicles in the metastatic process. *Biochimica et Biophysica Acta -Reviews on Cancer* **1869**, 64-77 (2018).
33. Becker, Annette, Thakur, Basant Kumar *et al.* Extracellular vesicles in cancer: cell-to-cell mediators of metastasis. *Cancer cell* **30**, 836-848 (2016).
34. Melo, Sonia A, Luecke, Linda B *et al.* Glypican-1 identifies cancer exosomes and detects early pancreatic cancer. *Nature* **523**, 177-182 (2015).

35. Toiyama, Yuji, Takahashi, Masanobu *et al.* Serum miR-21 as a diagnostic and prognostic biomarker in colorectal cancer. *Journal of the national cancer institute* **105**, 849-859 (2013).
36. Qu, J-L, Qu, X-J *et al.* Gastric cancer exosomes promote tumour cell proliferation through PI3K/Akt and MAPK/ERK activation. *Digestive liver disease* **41**, 875-880 (2009).
37. Miki, Yuichiro, Yashiro, Masakazu *et al.* Clinico-pathological significance of exosome marker CD63 expression on cancer cells and stromal cells in gastric cancer. *PloS one* **13** (2018).
38. Cufaro, Maria Concetta, Pieragostino, Damiana *et al.* Extracellular vesicles and their potential use in monitoring cancer progression and therapy: the contribution of proteomics. *Journal of Oncology* **2019** (2019).
39. Rupp, Anne-Kathleen, Rupp, Christian *et al.* Loss of EpCAM expression in breast cancer derived serum exosomes: role of proteolytic cleavage. *Gynecologic oncology* **122**, 437-446 (2011).
40. Davies, Ryan T, Kim, Junho *et al.* Microfluidic filtration system to isolate extracellular vesicles from blood. *Lab on a Chip* **12**, 5202-5210 (2012).
41. Nordin, Joel Z, Lee, Yi *et al.* Ultrafiltration with size-exclusion liquid chromatography for high yield isolation of extracellular vesicles preserving intact biophysical and functional properties. *Nanomedicine: Nanotechnology, Biology Medicine* **11**, 879-883 (2015).
42. Hong, Chang-Sook, Funk, Sonja *et al.* Isolation of biologically active and morphologically intact exosomes from plasma of patients with cancer. *Journal of extracellular vesicles* **5**, 29289 (2016).
43. Koga, Kenichiro, Matsumoto, Kotaro *et al.* Purification, characterization and biological significance of tumor-derived exosomes. *Anticancer research* **25**, 3703-3707 (2005).
44. Tauro, Bow J, Greening, David W *et al.* Comparison of ultracentrifugation, density gradient separation, and immunoaffinity capture methods for isolating human colon cancer cell line LIM1863-derived exosomes. *Methods* **56**, 293-304 (2012).
45. Kim, Chan Woo, Lee, Hwan Myung *et al.* Extracellular membrane vesicles from tumor cells promote angiogenesis via sphingomyelin. *Cancer research* **62**, 6312-6317 (2002).
46. Ghosh, Anirban, Davey, Michelle *et al.* Rapid isolation of extracellular vesicles from cell culture and biological fluids using a synthetic peptide with specific affinity for heat shock proteins. *PloS one* **9** (2014).
47. Lamparski, Henry G, Metha-Damani, Anita *et al.* Production and characterization of clinical grade exosomes derived from dendritic cells. *Journal of immunological methods* **270**, 211-226 (2002).
48. Nolte, Esther, Cremer, Tom *et al.* Extracellular vesicles and viruses: Are they close relatives? *Proceedings of the National Academy of Sciences* **113**, 9155-9161 (2016).
49. Sódar, Barbara W, Kittel, Ágnes *et al.* Low-density lipoprotein mimics blood plasma-derived exosomes and microvesicles during isolation and detection. *Scientific reports* **6**, 24316 (2016).
50. Ramirez, Marcel I, Amorim, Maria G *et al.* Technical challenges of working with extracellular vesicles. *Nanoscale* **10**, 881-906 (2018).
51. Chernyshev, Vasiliy S, Rachamadugu, Rakesh *et al.* Size and shape characterization of hydrated and desiccated exosomes. *Analytical bioanalytical chemistry* **407**, 3285-3301 (2015).
52. Van der Pol, Edwin, Coumans, Franck *et al.* Innovation in detection of microparticles and exosomes. *Journal of Thrombosis* **11**, 36-45 (2013).

53. Dragovic, Rebecca A, Gardiner, Christopher *et al.* Sizing and phenotyping of cellular vesicles using Nanoparticle Tracking Analysis. *Nanomedicine: Nanotechnology, Biology Medicine* **7**, 780-788 (2011).
54. Gamonet, Clémentine, Mourey, Guillaume *et al.* How to quantify microparticles in RBCs? A validated flow cytometry method allows the detection of an increase in microparticles during storage. *Transfusion* **57**, 504-516 (2017).
55. de Rond, Leonie, Coumans, Frank AW *et al.* Deriving extracellular vesicle size from scatter intensities measured by flow cytometry. *Current protocols in cytometry* **86**, e43 (2018).
56. Santilli, Francesca, Marchisio, Marco *et al.* Microparticles as new markers of cardiovascular risk in diabetes and beyond. *Thrombosis haemostasis* **116**, 220-234 (2016).
57. Pieragostino, Damiana, Cicalini, Ilaria *et al.* Enhanced release of acid sphingomyelinase-enriched exosomes generates a lipidomics signature in CSF of Multiple Sclerosis patients. *Scientific reports* **8**, 1-12 (2018).
58. Varga, Zoltán, Van der Pol, Edwin *et al.* Hollow organosilica beads as reference particles for optical detection of extracellular vesicles. *Journal of Thrombosis Haemostasis* **16**, 1646-1655 (2018).
59. Cappello, Francesco, Logozzi, Mariantonia *et al.* Exosome levels in human body fluids: a tumor marker by themselves? *European Journal of Pharmaceutical Sciences* **96**, 93-98 (2017).
60. Hoshino, Daisuke, Kirkbride, Kellye C *et al.* Exosome secretion is enhanced by invadopodia and drives invasive behavior. *Cell reports* **5**, 1159-1168 (2013).
61. Sauter, Edward R Exosomes in blood and cancer. *TRANSLATIONAL CANCER RESEARCH* **6**, S1316-S1320 (2017).
62. Carnell-Morris, Pauline, Tannetta, Dionne *et al.* Analysis of extracellular vesicles using fluorescence nanoparticle tracking analysis, in *Extracellular Vesicles* 153-173 (Springer, 2017).
63. Berne, Bruce J & Pecora, Robert *Dynamic light scattering: with applications to chemistry, biology, and physics*. (Courier Corporation, 2000).
64. Allison, David P, Mortensen, Ninell P *et al.* Atomic force microscopy of biological samples. *Wiley Interdisciplinary Reviews: Nanomedicine Nanobiotechnology* **2**, 618-634 (2010).
65. Vorselen, Daan, Marchetti, Margherita *et al.* Multilamellar nanovesicles show distinct mechanical properties depending on their degree of lamellarity. *Nanoscale* **10**, 5318-5324 (2018).
66. Park, Yong Hyun, Shin, Hyun Woo *et al.* Prostate-specific extracellular vesicles as a novel biomarker in human prostate cancer. *Scientific reports* **6**, 30386 (2016).
67. Moon, Pyong-Gon, Lee, Jeong-Eun *et al.* Fibronectin on circulating extracellular vesicles as a liquid biopsy to detect breast cancer. *Oncotarget* **7**, 40189 (2016).
68. Jiang, Ying, Shi, Muling *et al.* Aptamer/AuNP biosensor for colorimetric profiling of exosomal proteins. *Angewandte Chemie International Edition* **56**, 11916-11920 (2017).
69. Im, Hyungsoon, Yang, Katherine *et al.* Characterization of Extracellular Vesicles by Surface Plasmon Resonance, in *Extracellular Vesicles* 133-141 (Springer, 2017).
70. Whatley, Harry Basic principles and modes of capillary electrophoresis, in *Clinical and forensic applications of capillary electrophoresis* 21-58 (Springer, 2001).
71. Jorgenson, James W & Lukacs, KD Free-zone electrophoresis in glass capillaries. *Clinical chemistry* **27**, 1551-1553 (1981).

72. Jorgenson, James W & Lukacs, Krynn DeArman Capillary zone electrophoresis. *Science* **222**, 266-274 (1983).
73. Kraly, James, Fazal, Md Abul *et al.* Bioanalytical applications of capillary electrophoresis. *Analytical Chemistry* **78**, 4097-4110 (2006).
74. Tallarek, U, Rapp, E *et al.* Electroosmotic flow phenomena in packed capillaries: from the interstitial velocities to intraparticle and boundary layer mass transfer. *The Journal of Physical Chemistry B* **106**, 12709-12721 (2002).
75. Mironov, Gleb G, Chechik, Alexey V *et al.* Viral quantitative capillary electrophoresis for counting intact viruses. *Analytical chemistry* **83**, 5431-5435 (2011).
76. Cailleau, Relda, Olive, Matilde *et al.* Long-term human breast carcinoma cell lines of metastatic origin: preliminary characterization. *In vitro* **14**, 911-915 (1978).
77. Tang, Zheng-Hai, Jiang, Xiao-Ming *et al.* Characterization of osimertinib (AZD9291)-resistant non-small cell lung cancer NCI-H1975/OSIR cell line. *Oncotarget* **7**, 81598 (2016).
78. Foley, George E, Lazarus, Herbert *et al.* Continuous culture of human lymphoblasts from peripheral blood of a child with acute leukemia. *Cancer* **18**, 522-529 (1965).
79. Osteikoetxea, Xabier, Sódar, Barbara *et al.* Differential detergent sensitivity of extracellular vesicle subpopulations. *Organic biomolecular chemistry* **13**, 9775-9782 (2015).
80. Wu, Jiayan, Xiao, Jingfa *et al.* Ribogenomics: the Science and Knowledge of RNA. *Genomics, proteomics bioinformatics* **12**, 57-63 (2014).
81. Van der Waal, Isaäc Are we able to reduce the mortality and morbidity of oral cancer; some considerations. *Medicina oral, patologia oral y cirugia bucal* **18**, e33 (2013).
82. Lippman, Scott M, Sudbø, Jon *et al.* Oral cancer prevention and the evolution of molecular-targeted drug development. *Journal of clinical oncology* **23**, 346-356 (2005).
83. Carvalho, André Lopes, Nishimoto, Inês Nobuko *et al.* Trends in incidence and prognosis for head and neck cancer in the United States: a site-specific analysis of the SEER database. *International journal of cancer* **114**, 806-816 (2005).
84. Souchelnytskyi, Serhiy & Hanash, Sam Clinical Applications REPRINT. *Proteomics Clin. Appl* **3**, 116-134 (2009).
85. Tang, Haikuo, Wu, Zhiyuan *et al.* Salivary lncRNA as a potential marker for oral squamous cell carcinoma diagnosis. *Molecular medicine reports* **7**, 761-766 (2013).
86. Kalimuthu, Kalishwaralal, Kwon, Woo Young *et al.* A simple approach for rapid and cost-effective quantification of extracellular vesicles using a fluorescence polarization technique. *Journal of biological engineering* **13**, 31 (2019).
87. Amado, Francisco Manuel Lemos, Vitorino, Rui Miguel Pinheiro *et al.* Analysis of the human saliva proteome. *Expert Review of Proteomics* **2**, 521-539 (2005).
88. Buchholz, K Historical highlights and current status of biotechnology: From mystery to the lock and key hypothesis to the design of recombinant enzymes. *Medicinal chemistry research* **11**, 399-421 (2002).
89. Blank, A, Dekker, C *et al.* in Nucleic acids symposium series 203-209 (1981).

90. Fennoy, Sheila L, Jayachandran, Sanjay *et al.* RNase activities are reduced concomitantly with conservation of total cellular RNA and ribosomes in O2-deprived seedling roots of maize. *Plant physiology* **115**, 1109-1117 (1997).
91. Sniehotta, Maike, Schiffer, Eric *et al.* CE–a multifunctional application for clinical diagnosis. *Electrophoresis* **28**, 1407-1417 (2007).
92. Sekhon, Bhupinder Singh An overview of capillary electrophoresis: pharmaceutical, biopharmaceutical and biotechnology applications. *Journal of Pharmaceutical Education Research* **2**, 2 (2011).
93. Pascali, Jennifer Paola, Bortolotti, Federica *et al.* Recent advances in the application of CE to forensic sciences, an update over years 2009–2011. *Electrophoresis* **33**, 117-126 (2012).